Photometric Solutions for Semi-Detached Eclipsing Binaries: Selection of Distance Indicators in the Small Magellanic Cloud

J. S. B. Wyithe[1,2,4], R. E. Wilson[3]

ABSTRACT

Estimation of distances to nearby galaxies by the use of eclipsing binaries as standard candles has recently become feasible because of new large scale instruments and the discovery of thousands of eclipsing binaries as spinoff from Galactic microlensing surveys. Published measurements of distances to detached eclipsing binaries in the Large Magellanic Cloud combine stellar surface areas (in absolute units) determined from photometric light and radial velocity curves with surface brightnesses from model atmospheres and observed spectra. The method does not require the stars to be normal or undistorted, and is not limited in its applicability to the well detached systems that have traditionally been considered. We discuss the potential usefulness of semi-detached vis à vis detached eclipsing binaries for distance determination, and examine and quantify criteria for their selection from large catalogs. Following our earlier paper on detached binaries in the Small Magellanic Cloud (SMC), we carry out semi-detached light curve solutions for SMC binaries discovered by the OGLE collaboration, identify candidates for SMC distance estimation that can be targets of future high quality observations, and tabulate results of OGLE light curve solutions. We point out that semi-detached binaries have important advantages over well-detached systems as standard candles, although this idea runs counter to the usual view that the latter are optimal distance indicators. Potential advantages are that (1) light curve solutions can be strengthened by exploiting lobe-filling configurations, (2) only single-lined spectra may be needed for radial velocities because the mass ratio can be determined from photometry in the case of complete eclipses, and (3) nearly all semi-detached binaries have sensibly circular orbits, which is not true for detached binaries. We carry out simulations with synthetic data to see if

[1]Princeton University Observatory, Peyton Hall, Princeton, NJ 08544, USA

[2]Harvard-Smithsonian Center for Astrophysics, 60 Garden Street, Cambridge, MA 02138

[3]Astronomy Department, University of Florida, Gainesville, FL 32611

[4]Hubble Fellow

semi-detached binaries can be reliably identified and to quantify the accuracy of solutions. The simulations were done for detached as well as semi-detached binaries so as to constitute a proper controlled study. The simulations demonstrate two additional advantages for semi-detached distance determination candidates; (4) the well-known difficulty in distinguishing solutions with interchanged radii (aliasing) is much less severe for semi-detached than for detached binaries, and (5) the condition of complete eclipse (which removes a near degeneracy between inclination and the ratio of the radii) is identified with improved reliability. In many cases we find that parameters are accurately determined (*e.g.* relative errors in radii smaller than 10%), and that detached and semi-detached systems can be distinguished. We select 36 candidate semi-detached systems (although 7 of these are doubtful due to large mass ratios or periods) from the OGLE SMC eclipsing binary catalog. We expected that most semi-detached candidates would have light curves similar to those of common Algol binaries but that turned out not to be the case, and we note that fully Algol-like light curves are nearly absent in the OGLE sample. We discuss possible explanations for the near absence of obvious Algols in OGLE, including whether their paucity is real or apparent.

Subject headings: stars: eclipsing binaries – distances; galaxies: Magellanic Clouds; cosmology: distance scale

1. Introduction

Accurate measurement of the distances to the Magellanic Clouds is an important current issue as it provides a basic step toward determining the extragalactic distance scale. Paczynski (1997, 2000) has argued that eclipsing binaries now provide the most direct and accurate distances to the Magellanic Clouds, and examples are already in the literature (e.g. Guinan et al. 1998; Fitzpatrick et al. 2001). Recently, thousands of variable stars including eclipsing binaries have been discovered by the OGLE (Udalski et al. 1998), MACHO (Alcock et al. 1997) and EROS (Grison et al. 1995) collaborations as a by-product of galactic microlensing searches. These catalogs motivate a systematic, quantitative search for close to ideal systems for distance determination.

The method of measuring distances by means of eclipsing binaries has been known for decades, and its basis has been clearly explained by Paczynski (1997) and Guinan, et al. (1998), among others. In essence, light curves provide relative star dimensions (R_1/a, R_2/a, where R is mean radius and a is orbit size) and radial velocities establish the absolute scale

by providing the orbit size, so that one can find the R's in physical units by combining the two kinds of information. Fine effects, such as departures from sphericity, etc., can be modeled by modern eclipsing binary light curve programs. With absolute radii known, luminosities in physical units follow if emission per unit surface area (energy per unit area per unit time per wavelength interval) becomes known. Some persons favor calibrated relations based on interferometrically resolved, un-complicated stars for the emission measure while others favor the predictions of stellar atmosphere models that are fitted to spectral energy distributions (SED) of eclipsing binary distance estimation targets. Emission for plane-parallel atmospheres is determined, in principle, if effective temperature, log g, and chemical composition are specified. For a well observed eclipsing binary, g is computed to better than adequate accuracy as GM/R^2 and T_{eff} can be estimated by fitting a theoretical SED to an observed SED, as in Fitzpatrick & Massa (1999). In usual practice, surface chemical composition would be assumed normal, but that is the *only* normalcy assumption. The reasonableness of that assumption for *SD* binaries will be discussed below. The overall method is mainly geometrical, with only the emission measure involving radiative physics. It does not require knowledge of distances to calibration stars, as opposed to other standard candle methods such as by Cepheid variables or supernovae, and therein lies one of the primary advantages. Empirical calibration errors are bypassed if surface emission is computed from a stellar atmosphere model.

Although conventional wisdom holds that well-detached eclipsing binaries yield the most reliable light curve solutions, the basis for that conjecture may not extend beyond the scientific instinct that simpler is better. In fact there are real advantages to solutions of semi-detached (hereafter *SD*) and overcontact (*OC*) binary light curves, partly in the exploitation of lobe-filling configurations and partly through proximity effects, which provide information that is lacking in well-detached binaries. Actually, many factors influence the relative reliability of detached, *SD*, and *OC* light curve solutions. Accordingly, searches for standard candle binaries should examine all relevant considerations, including ones that argue for or against *SD* and *OC* systems. Here we consider *SD* binaries in the Small Magellanic Cloud (SMC) and will take up the *OC* case in a forthcoming paper. Our aims are to discuss the main considerations that bear upon the potential usefulness of *SD* binaries as standard candles, to identify good *SD* candidates for SMC distance determination via future observations with large telescopes, and to derive preliminary dimensional, radiative, and mass ratio properties of the candidates. Of course, *SD* binaries are fascinating objects in their own right, and we expect that their identification will also lead to investigations of *SD* properties unrelated to distance determination. SMC detached binaries were treated in Wyithe & Wilson (2001, hereafter Paper I).

The remainder of the paper is in four parts. Section 2 considers potential advantages

of *SD* binaries as standard candles. Sec. 3 discusses our automated fitting scheme and differences from the scheme described in Paper I for detached binaries. Quite apart from the logical arguments of Section 2, simulations can show statistically how well *SD* and detached solutions recover known parameters. This topic is discussed in Sec. 4. We also show how in some cases the issue of whether a binary is detached or *SD* can be determined from photometry with reasonable reliability. Sec. 5 has solutions to the OGLE catalog of eclipsing binary stars and discusses candidate *SD* binaries.

2. Conditions Relevant to the Use of *SD* Binaries as Standard Candles

Discussion of the measurement of distances to eclipsing binaries and their use as standard candles has traditionally centered around well detached systems. Measurements of distances to detached binaries in the Large Magellanic Cloud (LMC) have combined a stellar surface area (in absolute units) computed from photometric light and radial velocity curves with a surface brightness described by a model atmosphere to compute system luminosity (*e.g.* Guinan, *et al.* 1998; Fitzpatrick, *et al.* 2001). However surface brightnesses at all points over a stellar surface can be computed for nearly all classes of eclipsing binaries by combined use of modern eclipsing binary light-curve and model atmosphere programs. Therefore, it is not obvious that detached systems make the best eclipsing binaries for the purpose of distance determination. Indeed, as part of analyses of the fundamental parameters of *SD* binaries in the Magellanic clouds, Ostrov, Lapasset, and Morrell (2000; 2001) and Ostrov (2001) have already obtained preliminary values for the distance moduli. In this section we provide a general discussion of why we believe that many *SD*'s will turn out to be excellent standard candles. Of course, the use of *SD*'s for this purpose will need to be demonstrated for binaries with known distances, much as has been done in the case of detached binaries (Semeniuk 2000). This discussion also motivates our work on identification of *SD* systems in the OGLE eclipsing binary catalog in the sections that follow.

One can ask if it is a problem that most *SD* binaries have at least one significantly evolved star. The classical Algol *SD* binaries are abundant in the Milky Way and have other favorable characteristics, so we consider the question in the context of Algols. An Algol consists of a hot main sequence star that now is rather normal despite a history of growth by accretion, and a lobe-filling sub-giant that shows magnetic star spots and other magnetic and prominence activity, but is so dim as to contribute very little to system light. Basically the sub-giant acts as a moving mask that probes the primary via eclipses (although eclipses of the secondary by the primary also have some importance). The primary has regained nuclear and thermal equilibrium, following the accretion episode, and is now essentially a

normal main sequence star. Its composition usually is normal because the transferred gas came from the donor star's chemically normal envelope, not from it's chemically altered core. However there could be composition abnormalities in *SD* binaries that are not Algols, and these must be dealt with in individual cases. Typically there is some on-going mass transfer and emission line activity, but usually at a low level. Actually it may be difficult to see the emission lines, and they usually occupy only a minute fraction of an optical bandpass. Due to tidal circularization, Algols and other *SD*'s almost invariably have sensibly circular orbits, so evolution actually simplifies the standard candle problem in that regard. Accordingly, the evolved status of typical Algols does not disqualify them from serving as standard candles. Some Algols have disturbed light and radial velocity curves, but we seek only the best candidates and can discard questionable ones.

SD light curves are sensitive to mass ratio, $q = m_2/m_1$, thereby leading to the concept of a *photometric mass ratio*, q_{ptm}, in contrast with well detached binaries, whose light curves can be represented by a very wide range of q. The idea of a photometric mass ratio derives from that of limiting lobes and originated, in the *SD* case, with Kopal (1954; 1955). It works for both *SD*'s and *OC*'s, but *does not* work for detached binaries. The history of q_{ptm} for *OC*'s is more complicated and will be discussed in our forthcoming paper on *OC*'s. The basic explanation for *SD* q_{ptm} begins with the concept of a limiting (or critical) lobe as the volume within the largest closed equipotential that surrounds a member of a binary star system. The *SD* condition has the photosphere of one star accurately coincident with the surface of its limiting lobe, while the other star lies within its lobe. In Algols, the condition is maintained by continual slow expansion, accompanied by loss of matter through a nozzle around the null point of effective gravity that faces the companion star. A consideration that favors *SD* light curve solutions is that the lobe filling condition, when correctly recognized, mathematically eliminates a parameter, as it ties the nozzle location to mass ratio. That is, *SD* light curves contain information as to the location of star (and thus lobe) surface, so the lobe filling condition connects star size with mass ratio. Writing Ω_{cr} for (gravitational plus centrifugal) critical potential[5], we have a definite relation $\Omega_{cr} = \Omega_{cr}(q)$. The functionality can involve more parameters in unusual cases (*viz.* Wilson, 1979), but we limit our remarks to common synchronously rotating binaries with circular orbits. Naturally Ω_{cr} specifies the lobe filling star's size and figure. Thus Ω_{cr} and q become functionally related in a known way and the *SD* condition compresses the parameter space by an entire dimension. Of course elimination of a parameter will strengthen a solution by simplifying the parameter correlation matrix. The corresponding intuitive explanation for *OC*'s is best given somewhat differently, but formally

[5]Ω is a traditional dimensionless quantity that has the essential character of a potential, but differs from a true potential by an additive constant. It is defined so as not to depend on the absolute masses.

is the same - a functional relation eliminates one parameter dimension (*viz.* Wilson, 1994 for fuller explanations of the *SD* and *OC* cases). We mention a common mis-understanding, that q_{ptm} mainly derives from ellipsoidal variation (brightness undulation due to tidal distortion) - a notion that is essentially entirely wrong. It is the *size* of the lobe filling star, not its figure, that leads to q_{ptm}. Actually very little ellipsoidal variation is seen in most Algol light curves because the tidally distorted secondaries are very dim, yet q_{ptm}'s are found routinely and accurately for Algols.

In addition to overall solidification of solutions by the lobe filling condition, absolute star dimensions and masses can be found for *SD*'s having only single-lined spectra. Armed with knowledge of q from one or more light curves and of orbital semi-major axis a_1 from star 1 velocities, we trivially compute $a_2 = a_1/q$ without need for velocities of star 2. That point is particularly important for Algols, most of which have dim secondaries and therefore have spectra that are usually single-lined. Although not often available, a velocity curve for star 2 provides a check on q_{ptm}. A simultaneous light and double-lined velocity solution can extract consensus information (Wilson 1979) and solidify the solution. Systems with double-lined spectra may provide the best results, but the existence of q_{ptm} means that we are *not dependent* on double-lined spectroscopy.

As mentioned in the introduction the surface brightness, needed to compute luminosity and hence distance, can be computed either from calibrated relations (based on interferometrically resolved, un-complicated stars) or from the predictions of stellar atmosphere models that are fitted to binary SED's. An important distinction is that if one requires empirically calibrated stellar surface brightnesses, then attention must be limited to cases of well detached binaries containing undistorted *normal* stars. However, the use of stellar atmosphere models removes this restriction, and enables the use of binaries containing evolved and/or tidally distorted stars, and hence the harnessing of the better constrained solutions offered by *SD* binaries. Evidence of the applicability of stellar atmosphere models was provided by Ribas et al. (2000) who simultaneously solved for component temperatures, metalicity and surface gravities as well as interstellar reddening (using the scheme of Fitzpatrick & Massa, 1999) as part of a measurement of the distance to HV 2274 in the LMC. Ribas, *et al.* found a surface gravity in good agreement with that from their simultaneous light - velocity solution with the Wilson-Devinney model, and metalicities in good agreement with those for the LMC, which lends confidence that the method is working correctly.

Another point to be taken into account is that completely eclipsing (*i.e.* total-annular) systems give much better results than partially eclipsing ones, basically because there is little tradeoff between inclination and other parameters for complete eclipses. Also, a *moderate luminosity ratio* helps in two ways - by improving the quality of (and chances for) secondary

star velocities and by making the secondary eclipse reasonably deep. *Moderate mass ratios* are good in that they produce reasonably large primary star velocity amplitudes.

In summary, this section discussed the value of *SD* binaries as standard candles, where important advantages are that a light curve can tell the mass ratio, that light curve solutions involve one fewer parameter than do detached solutions, and that circular orbits are the rule. Knowledge of q_{ptm} allows full absolute dimensions (and masses) to be derived for a binary with *single-lined* spectra, in contrast with the detached case, where double-lined spectra are necessary. In cases where the spectra are double-lined, redundancy in the determination of the mass ratio will further strengthen solutions. There is a downside in the case of common Algols: although velocity curves for the primaries should be measurable (it is by far the brighter component), the curves will have small amplitude because star 1 is much the more massive component. Thus the principal observational need is outstandingly accurate radial velocities. For the SMC, that requirement involves large telescope aperture and an excellent radial velocity spectrograph but it can be done, especially if *large numbers* of velocities are measured so as to average out the noise. The problem of small primary velocities does not apply to all *SD*'s, and not even to all Algols, but does apply to most of the common Algols.

The advantages mentioned above relate to the potential improvement of light-curve solutions and corresponding distance determinations from *SD* binaries relative to detached binaries. *SD*'s usually have comparatively robust solutions with smaller parameter uncertainties, an outcome that should lead to more accurate distance estimates and provide motivation to identify candidates in survey data - the subject of the remainder of this paper. We shall learn about other advantages from the simulations of Sec. 4 that relate to the *identification* of candidates for detailed follow up observation. These include reduced incidence of false solutions with reversed primary and secondary radii that lead to incorrect initial estimates of luminosity ratios (thereby wrongly predicting whether spectra are double or single-lined), and improved identification of complete eclipses. Furthermore, we shall show that observation of *SD* binaries will be a relatively efficient use of resources due to reliable initial determination of system properties.

3. The Fitting Scheme

In the interest of completeness, we outline the automation procedure that was fully described in Paper I and is built around public light curve (*LC*) and differential corrections (*DC*) FORTRAN programs (Wilson and Devinney, 1971; Wilson, 1979, 1990, 1998; hereafter WD program or WD model). *LC* computes light and radial velocity curves and also spectral line profiles and images of binary stars, including effects of tides, mutual irradiation, spots,

eccentric orbits, and other effects. Star surfaces are specified in terms of equipotentials. *DC* accepts observed data and parameter estimates and computes corrections to the estimates according to the Least Squares criterion. The distributed version of *DC* does only one iteration per submission so as to ensure human interaction in the progress of a solution. The automation shell that renders processing of thousands of binaries practical is a PERL script that loops the *DC* iterations, tests for proper convergence, and generates light curves with *LC*. The *LC* and *DC* programs work in eight operational modes that mainly relate to morphology, with detached, *SD*, *OC*, etc. configurations represented by corresponding modes. Here we use only mode 2 (detached), where there is no constraint on the surface potentials, and mode 5 (*SD*), where the secondary star potential is required to be exactly that of the lobe.

Initial parameter estimates are those of the best match in a pre-computed library of light curves, with separate libraries for modes 2 and 5. Naturally the actual time scale is likely to need some shifting to optimize a match with a given binary, whether it be synthesized or real (from OGLE). As in Paper I, we begin by adjusting the reference epoch (t_0) while keeping the Udalski et al. period. We then compare a given observed light curve with each one in the appropriate library of simulated systems to find the closest Least Squares match. The flux scale is controlled by L_1, the bandpass luminosity of star 1, which acts only as a scaling factor because fluxes are not on an absolute scale at this stage of analysis.

Our basic strategy for *SD*'s differs from that for detached binaries: instead of entering a *fixed* q and relying on the fact that detached light-curves are insensitive to q, we *solve* for q in the *SD* case. Converged parameters for *SD* binaries are Ω_1 ("potential"), T_1 (mean surface temperature), i (inclination), q, and L_1. t_0 and e (orbital eccentricity) are adjusted but convergence of these parameters is not a solution requirement. e is expected to be 0 for *SD* systems, and is adjusted in the interest of experimentation. ω (the argument of periastron) is distributed between 0 and π, but is fixed at the value of the initial guess. Of course, Ω_2 is set by q for *SD* systems. For detached solutions, which we need for comparison purposes, Ω_2 is a parameter but q is not, as q cannot ordinarily be found for detached solutions (*viz.* Paper I for remarks on experiences with convergence of mode 2 solutions). Detached systems can have larger e's, and we found that more accurate solution parameters were obtained where ω was restricted to 0 or π.

DC convergence is improved by application of the well known Levenberg-Marquardt scheme (Levenberg, 1944; Marquardt, 1963) with factor $\lambda = 10^{-5}$, and also by the Method of Multiple Subsets (MMS, Wilson and Biermann, 1976). Iterations ended when all corrections to parameters for which convergence was required were below 0.2 times the standard errors from auxiliary solutions of the full parameter set. There were two *groupings* of subsets,

with the second grouping as back-up in case the first grouping failed to converge or led to an unphysical solution. For *SD*'s, where eccentric orbits are a rarity, another two subset groupings were used as back up. Using this second pair e was fixed at the value of the initial guess in addition to fixing ω. The subset groups are summarized in Tab. 1 for both *SD* and detached systems.

The method for finding *SD* solutions for eclipsing binaries in the SMC is similar to that for the detached binaries of Paper I, but with some differences. By far the most important difference is that we constrain one star to be in accurate contact with its limiting lobe, and accordingly can learn q from a well conditioned light curve. Phasing, weighting, limb darkening, and radiative physics are handled in the way of Paper I, while the manner of treating mass ratio is changed, as is that of handling the lobe configuration. Briefly, phasing has star 1 eclipsed near phase zero (where we ordinarily find the deeper eclipse), weighting assumes that scatter scales with the square root of light level, and limb darkening has $I/I_0 = 1 - x(1-\mu) - y\mu \ln \mu$ with μ the cosine of the angle from the surface normal. Intensities I are averages over the photometric I-band (the most extensive OGLE light-curves were observed in I-band). Limb darkening coefficients x, y were fitted to Kurucz (1991) model stellar atmospheres by Van Hamme (1993). Colors reported by Udalski et al. (1998) indicate typical spectral types of O and B. However only relative temperatures T_1 and T_2 matter for single band light curves so we assumed fixed T_2's of $10,000K$ (with the black body radiation law) and allowed the program to find the T_1's. Limb darkening is demonstrably unimportant for noisy light curves so we assumed $x = 0.32$ and $y = 0.18$ for all binaries, with the numbers from Van Hamme (1993) for $15,000K$ and the I band. The model can do either a simple or a detailed reflection computation (Wilson 1990). To reduce computing time, we chose the simple law (MREF=1), which should be thoroughly adequate here. Bolometric albedos were unity and the stars were assumed to rotate synchronously and had no spots. Although low temperature Algol type secondaries will have convective envelopes and consequently have low albedos of ≈ 0.5 (Rucinski, 1969), assignment of albedos on a case by case basis can be done later, for solutions of accurate future light curves. The treatment of orbital eccentricity and argument of periastron is somewhat problematic and was discussed in Paper I for the detached case. All *SD* solutions for OGLE binaries that were finally accepted have e's consistent with zero. Tests of a representative sample of OGLE light curves showed that the light of any hypothetical third star was typically not detectable, so we fixed third light (l_3) at zero. However the issue of third light can be important and the possibility of its existence will have to be examined for individual distance modulus candidates when accurate photometry and spectroscopy is carried out. Candidates suspected of having a significantly bright third star will probably have to be rejected. Note that Algol itself has such a third star. The parameters and control integers described above that govern the operation of *LC* and *DC*

are summarized in Tabs. 2 and 3.

Our testing procedure simulated and solved not only *SD*'s but also detached binaries, so that proper comparisons could be made. We tried two configurations for every detached binary, each with its own pre-computed library. The simulated systems in one of these libraries are like main sequence binaries, with the hotter star (star 1) larger and more massive. The second library shows differential evolution, with the higher mass star having expanded and cooled so as to have a lower temperature than its companion. However, although evolution has switched the stars' roles in terms of temperature, it has not (yet) led to lobe filling, so we still have a detached binary that has not experienced mass reversal. In terms of real evolution, the lower mass star may also be significantly evolved if the masses are nearly equal, or may be essentially unevolved if the masses are substantially unequal. The condition with nearly equal masses and "double evolution" can be identified with the RS CVn type binaries that populate eclipsing binary catalogs in large numbers (Morgan and Eggleton, 1979). We adopt the better of the two solutions in the Least Squares sense, at the stage of the initial guess for each binary. In terms of rejecting aliased[6] solutions, this approach was found to be as successful as one where a fully converged solution was computed in each case. Classification of the solution at the stage of the initial guess halves the computation time.

4. Tests with Simulation Catalogs

We applied our fitting algorithm to simulated catalogs of *SD* and detached binaries. The objectives were to check *DC*'s error estimates, assess systematic error due to assumptions of fixed parameter values, and investigate the success rate in distinguishing *SD* from detached binaries.

4.1. *SD* solutions for simulated *SD* binaries

We simulated 120 *SD* eclipsing binaries. Each binary had 150 randomly spaced synthetic observations (typical of OGLE binaries), and Gaussian noise that scales as the square root of light level, referenced to 5 percent noise at mean light. Each system has T_1 between $15,000$ and $30,000K$ and $T_2 = 15,000K$. Notice that the T's may not be representative of the most common Algols, being rather high and insufficiently different. The resulting moderate surface brightness ratios produce deep secondary eclipses, and relatively strong solutions. It

[6]We define aliased solutions as those with interchanged radii.

turns out (Sec. 5) that most of the *SD*'s that we find are *not* typical of the common variety of Algol, such that the simulation catalog temperatures are reasonably representative.

Limb darkening coefficients are from Van Hamme (1993) for the adopted temperatures. The simulation catalog had q's between 0.01 and 10.0. While Algols typically have q's of a few tenths, this larger range allows for the possibility of selecting objects in a different stage of evolution. The simulated binaries had assorted inclinations and (star 1) surface potentials. Eccentricities in the range 0.0 to 0.1 (with $\sim$ 80 percent below 0.03) were assumed. This range of eccentricities is smaller than that assumed for detached binaries in Paper I, reflecting the expectation that evolved binaries should have circularized orbits. The selection of *SD* binaries from the OGLE catalog (Sec. 5) will require e's consistent with zero.

The upper two rows of Fig. 1 show 10 of the simulated *SD*'s, as fitted in *SD* mode (mode 5). Acceptable solutions were obtained for 118 of the 120 simulated *SD*'s. The lower two rows show the same synthesized *SD* data fitted in detached mode (mode 2) and will be discussed in Sec. 4.5. Fig. 2 shows the reliability of parameter extraction for r_1 and q, with standard error bars Δr_1 and Δq, in terms of both direct comparison and residuals (throughout this paper r refers to the polar radius in units of the orbital semi-major axis). The figure demonstrates that the fitting scheme accurately recovers those parameters without bias, and that the standard errors from *DC* fairly represent statistical uncertainties. The errors are essentially normally distributed over the full range of error sizes and do not show a large tail (39% and 14% of values lie beyond 1σ and 2σ). Fig. 3 shows solution values vs. known values for several other parameters. Values for $r_1 + r_2$, r_1/r_2 and L_1/L_2 are very accurately reproduced, while i, e and mean surface brightness ratio (hereafter J_1/J_2) are also reliably recovered.

In Paper I we defined the quantity, valid for circular orbits:

$$F_e \equiv \frac{r_l + r_s - \cos i}{2r_s}, \tag{1}$$

which is greater than unity for systems with complete eclipse (strictly true only for spherical stars, but nearly true otherwise). Here r_l and r_s are the polar radii of the large and small stars in units of orbital semi-major axis, a. Fig. 4 shows F_e for the simulated binaries vs. the corresponding solution values, with regions of complete and partial eclipse distinguished for both the simulated binaries and their solutions. This plot demonstrates that F_e is recovered reasonably accurately for *SD* systems. In particular, the eclipse condition is correctly predicted in 95% of cases, based on the value of F_e. Reliability of F_e test applications will be greatly improved for the high quality light curves one can expect from observations with large telescopes. Recovery of F_e in the simulations gives confidence that solutions of real binaries can be properly identified as to type (complete vs. partial).

4.2. detached solutions for simulated detached binaries

We generated 120 simulated detached binary systems in analogy with the sample described in Sec. 4.1, with the potential of star 2 now independent of mass ratio and separately distributed. Differences related to evolution were discussed in Sec. 2.1. The upper panels of Fig. 5 show examples of mode 2 fits to the simulated detached systems. Detached solutions were obtained for 116 of the 120 simulated systems. Figs. 6, 7, and 8 serve the same purpose for the detached systems as do Figs. 2, 3, and 4 for the *SD* systems - comparison of solution values with known values. There are significant systematic departures from expected patterns. A well-known phenomenon, especially for partial eclipse light curves, is that a solution with the radii interchanged may give essentially the same quality of fit as one with the correct radii. We call this phenomenon *aliasing*. Aliased solutions make up about 25 percent of the sample. For the non-aliased solutions (shown by the solid dots in Figs. 6 and 7), the fitting scheme does well in recovering input model radii, the errors provide a good description of precision, and no significant systematic errors are apparent. This result is clearly demonstrated by the lower panels of Fig. 6 that show $|r - r_{sim}|/\Delta r$ plotted against the absolute size of the error, Δr. The aliased solutions, recognized as those having r_1/r_2 inverted with respect to the simulated binary and with both radii significantly wrong, are plotted as diamonds in Figs. 6 and 7. Fig. 6 shows systematic departures in both directions for r_1 and r_2 in the aliased solutions.

Fig. 7 shows derived vs. correct values for $r_1 + r_2$, r_1/r_2, J_1/J_2, L_1/L_2, i, and e. The sum of radii is very accurately reproduced, while J_1/J_2 and i are also reliably recovered for both aliased and non-aliased solutions. However major error is clearly present for r_1/r_2 and L_1/L_2 from aliased solutions. Aliasing is the dominant source of systematic error for the data set as a whole. The ratio of radii is reasonably well reproduced in non-aliased solutions. The eccentricity is often not recovered, and has unrealistic standard errors because the error is completely dominated by the assumption that ω is 0 or π. The fitted e is a lower limit.

Fig. 8 shows F_e for the simulated detached solutions vs. known F_e, with regions of complete and partial eclipse distinguished for both the simulated binaries and their solutions. Due to aliasing errors in i and r_1/r_2, the solution F_e's are often very poorly reproduced. Most notable are the degraded results for detached binaries compared to the *SD*'s of Fig. 5. However, solutions with $\Delta r_1/r_1 < 0.05$ and $\Delta r_2/r_2 < 0.05$ (large dots) reliably determine the condition of complete or partial eclipse.

4.3. *SD*'s and the aliasing problem

The statistics of the aliasing problem, in which solutions with interchanged radii fit about equally well, are effectively shown by Figs. 2, 3, and 4 (*SD* solutions of *SD*'s) and Figs. 6, 7, and 8 (detached solutions of detached binaries). Clearly the problem is considerably less serious for *SD*'s than for detached systems, and constitutes a further important advantage for the selection of *SD*'s to be used as ideal distance indicators. This is because, while the relative star sizes may appear equally well determined in the correct and aliased solutions, the luminosity ratio can be very different for systems with unequal radii and temperatures. Therefore, until high-quality follow up photometry is obtained, selection of systems with moderate luminosity ratios (to facilitate observation of double-lined spectra) can be made confidently only for *SD* binaries.

We now ask if that situation can be understood in simple terms. Notice that although the members of a well-detached binary may differ in surface brightness, *they are twins in figure* (both nearly spheres) and, with regard to the solution, *mass ratio is irrelevant*. In particular, contributions to ellipsoidal variation in a well-detached binary are small and comparable for the two stars, so interchanging the radii has nil effect on ellipsoidal variation. In *SD*'s, however, the contact component has practically all of the tidal distortion, so the ratio of radii (which controls the ratio of luminosities) can have some importance. For example, if we make the contact star larger, it will necessarily be more luminous and impress more ellipsoidal variation on the light curve. Figs. 2, 3, and 4 demonstrate that the difference in ellipsoidal variation is sufficient to reduce the severity of aliasing in the *SD* case.

4.4. the relative quality of *SD* and detached solutions for survey quality data

Solutions for $r_1 + r_2$ and J_1/J_2 are of comparable quality for *SD* and detached binaries. The solutions for r_1 and r_2, and therefore r_1/r_2 and L_1/L_2 for detached systems suffer from aliasing, while these quantities are more reliably recovered for *SD* binaries. In Paper I, the degeneracy between i and r_1/r_2 for partially eclipsing detached binaries was discussed in detail. The more accurate recovery of i, aside from aliasing effects, indicates that this degeneracy is not as strong for *SD* binaries. Furthermore, recovery of i and r_1/r_2 leads to the accurate recovery of F_e. Thus Figs. 3, 4, 7 and 8 demonstrate those two further important advantages for the selection of *SD* systems that will be suitable for distance indication. For given light-curve quality, identification of complete eclipses is more robust for *SD*'s. Complete eclipses are important for both detached and *SD* binaries since they lead to accurate, robust solutions, and hence an accurate distance. For *SD*'s, this condition can be immediately identified with good reliability, without having to obtain further, high

quality light-curves. In addition L_1/L_2, which governs whether the system will have single or double-lined spectra, can be more accurately predicted.

4.5. can light curves distinguish *SD*'s from detached binaries?

SD light curves can resemble those of detached systems and vice-versa, as demonstrated in the lower two rows of Figs. 1 and 5. In an effort to quantify the problem, the simulated *SD*/detached systems were fit in reversed modes (detached /*SD*) (Fig. 1 / Fig. 5), in addition to the normal way. A detached solution was obtained for 107 of 120 simulated *SD*'s. Mode 2 can mimic the light-curve of an *SD* system, but typically Ω_2 is very nearly critical. A small adjustment can therefore move the solution outside the physically allowable range before convergence, resulting in failure to obtain a solution. Aliased solutions were found as for the simulated detached binaries. The detached solutions can both over and under-estimate r_2. However the detached solutions tend to overestimate the sum of the polar radii systematically. This is expected if the solution essentially finds a correct *mean* radius for the lobe filling star, as detached stars are less distorted than lobe filling components. There appears to be no systematic dependence on solution mode for r_1/r_2, i or J_1/J_2. In the converse situation, *SD* solutions were obtained for 109 of 120 simulated detached systems. In this case, failures tend to result from convergence to a solution with residuals larger than the scatter. The *SD* solutions again can both over and under-estimate r_2. There was no obvious systematic dependence on solution mode for $r_1 + r_2$, r_1/r_2, or J_1/J_2. However the *SD* solutions tend to underestimate i systematically for detached binaries.

Fig. 9 illustrates success in determining whether a system is *SD* or detached, based on the light-curve residuals. Each simulated binary (from both the *SD* and detached catalogs) has a point in one (and only one) of the three panels, and simulated *SD* and detached binaries are marked by diamonds and dots respectively. Simulated binaries with both *SD* and detached solutions are in the central panel, where the ratio of the sum of the squares of residuals (detached/*SD*, hereafter the *SS* ratio) is plotted against $r_1 + r_2$. A reasonable fraction (34%) of systems with both *SD* and detached solutions have *SS* ratios outside the region of statistical overlap and can be reliably classified on that basis. The lower panel shows 10 simulated systems having only a detached solution and 2 misclassified objects. Similarly the top panel shows 13 simulated systems having only an *SD* solution and 3 that have been misclassified.

It is important to emphasize that later high quality data from large telescopes will allow recognition of *SD*'s much more reliably than do OGLE data, from which we seek only *candidates* for follow-up observations. A consistency check will exist where double-lined

spectra are available, for then one can compare q_{ptm} from *SD* light curve solutions with q from radial velocities (q_{rv}). One expects that q_{ptm} will be smaller than q_{rv} for detached systems (the detached q_{ptm}'s being wrong) and that the two q's will agree for *SD*'s. There is some help from *SD* solutions even for binaries with single-lined spectra, because a good q_{ptm} should lead to plausible absolute masses for an *SD* system and implausible ones for a detached system. For examples of high quality data in programs dedicated to individual Magellanic Cloud eclipsing binaries (binaries observed with a 2.15 m. telescope), see Ostrov, Lapasset, and Morrell (2000) and Ostrov (2001). One can expect even better data collections with the larger telescopes and future intensive observing justified by the Magellanic Cloud distance problem. Ribas, *et al.* 2000 similarly treated the bright LMC eclipsing binary HV 2274 with a telescope of only 0.61 m. aperture.

5. OGLE SMC Binaries - Recognition and Solutions

The OGLE catalog was recorded automatically and is therefore essentially free of selection effects, except for those imposed by limiting magnitude ($I \lessapprox 20^m$), by period range ($0.^d3$ to 250^d), and by precision (which depends on brightness, *viz.* Udalski, et al., 1998). Most important is that OGLE stars were not selected according to observer interest, observational convenience, or horizon location. Accordingly the catalog is an important new resource not only for distance estimation but also for binary star statistics, as are the EROS and MACHO catalogs. However those two purposes are linked because distance estimation requires reliable recognition of category membership, which in turn should be checked against expected category statistics. The first 30 systems from OGLE field 2 are illustrated in Fig. **??** (with *SD* solution fits), so as to give an impression of typical light curves rather than selected ones. An even better overview can be attained by inspection of the 1459 light curve panels in Udalski et al. (1998).

The most easily recognizable *SD* binaries in our Galaxy are of the Algol type, such as Algol, TW Draconis, U Sagittae, and S Equulei, to mention a few. A distinction is made among classical Algols, short-period Algols, and "pseudo-Algols" (our term). Classical Algols are understood to have experienced an episode of rapid and large scale matter transfer that has now ended, followed by a long-lived *SD* state of slow transfer. Compared to many other categories of extrinsic and intrinsic variable stars, they form a category with very good evolutionary coherence. These are the only "Algols" for which one can assume an *SD* state with confidence. The short period Algols ($P \lessapprox 1$ day) are a mixed bag of uncertain status, containing some classical Algols, some slightly detached main sequence binaries, and even some erstwhile *OC* systems that have temporarily broken contact. The third cate-

gory, pseudo-Algols, is primarily composed of main sequence detached binaries with very unequal (primary vs. secondary) temperatures, although a minority are bizarre products of moderately advanced evolution. That is, pseudo-Algols are simply mis-typed, although some catalogs of Algols have them in large numbers, as their light curves superficially resemble those of (classical) Algols. Evolved pseudo-Algols are likely to be *SD*, but with more complicated histories than classical Algols.

The signature light curves, by which all of these categories are assigned the name *Algol type,* have deep primary and shallow (in extreme cases, nearly undetectable) secondary eclipses. There usually is some variation between eclipses due to the "reflection" effect and tidal deformation, but typically with $\lessapprox 0^m.1$ amplitude. Among the three "Algol" categories, classical Algols conform best to the above light curve description and can thereby be rather reliably recognized, provided that the inclination is high (say $> 80°$) and the period is longer than a day or so.

Curiously, remarkably few OGLE light curves resemble those of the common classical Algols, which should be abundant according to experience with Milky Way binaries. Typically, the OGLE secondary eclipses are comparatively deep or there is too much variation between eclipses, or both conditions occur. Reasons to consider are:

• Could Milky Way binary statistics be biased in favor of finding "normal" Algols, perhaps observationally or according to the interests of observers? Might there even be a bias according to what becomes published? Unfortunately, existing statistical compilations do not reliably distinguish classical Algols from Algol look-alikes. Resolution of these issues would be an interesting project, but is beyond the scope of this paper.

• Could OGLE SMC statistics be biased against finding "normal" Algols? Certainly there is no bias against period, as Algol periods lie well within OGLE limits. Algols with primaries of spectral types middle A and later might be too faint for the OGLE limiting magnitudes, but B-types should be readily observable. Detection of the deep eclipses of Algols is assured, given OGLE's precision. Therefore, although this possibility might explain a substantial deficiency of Algols, it would not seem to explain their near absence in OGLE. By eye we see only about 20 of the 1459 light curves that might resemble those of common Algols, and only about 5 appear entirely normal.

• Could we be misled by the printed OGLE light curves being for the I band, while most light curves in journals are for V or B? Indeed, I band curves will have deeper secondary and shallower primary eclipses, as well as increased ellipsoidal variation, compared to shorter wavelength bands. Although these effects are in the right sense, one can make approximate allowances, and they seem insufficient to account for OGLE's apparent shortfall in normal

Algol light curves.

• Could Algols be far less abundant in the SMC than in the Milky Way? At first sight this seems unlikely, but it must be considered, given that several other kinds of objects differ statistically between the SMC and Milky Way. For example, Algol formation could be sensitive to chemical composition, given that a proper physical and quantitative theory of Algol formation does not exist.

• A minor point is that what appear to be alternating eclipses of equal depth may in some cases be successive primary eclipses, with undetectable secondaries in between and the period being half of that assumed. However that possibility could add only a few Algols, at most.

Note that we do not require that our *SD*'s be Algols, and certainly not necessarily Algols of the most ordinary kind. It is just that one expects ordinary Algols to be the most abundant *SD*'s, yet very few OGLE light curves resemble those of the familiar classical Algols.

Strong tidal dissipation associated with lobe filling causes the vast majority of *SD*'s to have circular orbits, so eccentricity is a very useful practical discriminant by which to filter out non-*SD*'s (lobe filling for an eccentric binary basically means that the lobe is filled at periastron). We shall rely on the *SS* ratio test and absence of eccentricity to identify *SD* systems and defer to later the issue of how many OGLE *SD*'s can be considered Algols.

5.1. *SD* and detached solutions for SMC binaries

Now having some experience with simulated *SD* binaries and with the "normal Algol" issue put aside, we applied our algorithm to the OGLE catalog and found *SD* and detached solutions for 92 percent and 88 percent of eclipsing binaries, respectively. We found solutions of both kinds for 83 percent.

Figs. 10-12 give an overall impression of the *SD* solution statistics for all systems in all the SMC fields and demonstrate the range of solutions and range of solution quality in plots of r_1 vs. r_2 (Fig. 10), q vs. r_1 (Fig. 11), and L_1/L_2 vs. J_1/J_2 (Fig. 12). A dearth of binaries with $r_1 \approx r_2$ appears as a gap that is not found in corresponding plots for simulated binary catalogs, and is therefore not an artifact of the analysis. The gap also appears in the q statistics, but again not in plots for simulated binary catalogs. Classical Algols would be found in the upper right hand corner of the plots in Fig. 12. The range of solutions for q, L_1/L_2, and J_1/J_2 is comparable to that of the simulated *SD* catalog.

The range and quality of detached solutions for r_1 and r_2 are shown in Fig. 13 (see also

Paper I). The dearth of $r_1 \approx r_2$ *SD*'s in Fig. 10 is not seen in the detached results. The range of solutions for r_1 and r_2 is comparable to that of the simulated detached catalog.

5.2. Selection of candidate *SD* OGLE binaries

Ratios of *SS* between detached and *SD* OGLE solutions are plotted against r_1+r_2 in Fig. 14, corresponding to Fig. 9 for the simulated binaries. We found from Fig. 9 that systems with a solution in only one mode do not have their condition reliably predicted by that mode. That is, although the successful solution mode correctly predicts a system's morphological type in most such examples, there are too many exceptions for confident assessment. Both main sequence and RS CVn type binaries may be significant contaminants in selection of *SD* binaries from the upper panels of Fig. 14. RS CVn's are abundant detached binaries that have evolved beyond the main sequence. The more massive star is larger and cooler and periods range from about 2 days to 2 weeks.

Of the binaries that have solutions in both *SD* and detached modes, 6 percent have *SS* ratios greater than 1.1, and 30 percent have *SS*< 0.95. Our selected *SD*'s have solutions in both *SD* and detached mode and *SS* ratios > 1.1. Fig. 14 shows that our fitting algorithm is more likely to fail in mode 2 when $r_1 + r_2$ is large, and in mode 5 when it is small. However solutions are found over a wide range of $r_1 + r_2$. We found no trend of *SS* ratio with system brightness. In particular, bright binaries are not preferentially selected as *SD*, based on the *SS* ratio criterion.

Figs. 15 and 16 show *SD* light curve fits for OGLE binaries selected from the requirement that $e < 3\Delta e$ and from the *SS* ratio criterion. Of the objects having *SS*>1.1, 50 percent had e inconsistent with zero. Most of the systems rejected on this basis had solutions for mass ratio larger than or around 1, consistent with their being detached objects, but having the more massive component evolved, or even being of RS CVn type. The solutions are summarized in Tab. 4. The first 13 systems are completely eclipsing according to the $F_e > 1$ criterion and are among the best candidates for distance determination. Fig. 17 shows r_1 vs. r_2, q vs. r_1, and L_1/L_2 vs. J_1/J_2 for systems judged to have complete (diamonds) and partial (dots) eclipses. The figures and Tab. 4 demonstrate that the instances of complete eclipse result from r_2 being larger than r_1, from larger q's, and from larger i's. Most of the systems have q's of a few 10ths to 1, so the primaries will have significant *RV* amplitudes.

Both completely and partially eclipsing *SD*'s were selected over a surprisingly large range of mass ratio. Systems 4-91631 and 5-190577 have $q > 10$, and 9-59110 has $q = 1.96$. These have the smallest r_1's as well as the smallest L_1/L_2 and could possibly be *SD* binaries

in the early stages of mass transfer. However the light curves are not erratic, as would be expected for rapid mass transfer, so they are more likely to be evolved but detached systems. If so these stars are very unusual astrophysically and worth observing as objects of special interest, aside from distance determination.

The majority of systems have luminosity ratios of several 10ths to 1, indicating that their spectra will be double-lined. However two objects (3-213548 and 9-163573), have large luminosity ratios, q's of ≈ 0.03 and surface brightness ratios of 3.0 and 1.8. These (particularly 3-213548) are the objects most likely to be classical Algols (as is apparent from their light-curves, although 9-163573 has very shallow eclipses). The near absence of normal Algol light curves in the OGLE catalog was discussed at length at the beginning of this section. Their near absence in our candidate list is therefore not due to the selection criterion. Of the 5 systems with light-curves (selected by eye) that most resemble those of classical Algols, 4-131230, 8-20567 and 5-283889 had *SS* ratios near 1, and 5-289333 and 6-200243 had $SS > 1.1$, but statistically non-zero e's.

Fig. 18 shows color-period and color-magnitude diagrams for all 36 candidate *SD* OGLE binaries, superimposed on the whole OGLE eclipsing binary catalog. The candidate *SD* binaries have color, magnitude, and period distributions similar to those of the whole catalog. Most have colors of hot main sequence stars. A few have redder colors, suggesting that the evolved component still contributes a significant fraction of total light. The two objects with very large q's do not have overly red colors, but the completely eclipsing system with $q = 1.96$ has V-I= 0.91. Most of the candidate *SD* binaries have periods of a few days, consistent with typical Algol periods, although most of the light curves are not typical of Algols. Those binaries with longer periods also have redder colors and are the least likely *SD* candidates.

6. Conclusions

Although traditionally used, well detached eclipsing binaries are not necessarily the ideal or only choice for eclipsing binary distance determination, since absolute brightnesses on absolute stellar surface elements can be computed and integrated over surfaces for almost all classes of eclipsing binaries. In this paper we have presented arguments in support of semi-detached (*SD*) eclipsing binaries as standard candles, and taken this as motivation to find *SD* solutions to the OGLE SMC eclipsing binary catalog, and to select *SD* systems for future study.

Several advantages of *SD* binaries, in particular the exploitation of lobe-filling configu-

rations lead to accurate light-curve solutions and may therefore lead to accurate distances. However before investing the considerable effort to make the observations required for a distance determination, it is helpful to have confidence that the binary is appropriate for the purpose. We have found several advantages for *SD* systems that relate to the selection of candidates from the large catalogs of light-curves now becoming available. We find that aliased solutions (where the radii are interchanged) are significantly less of a problem for *SD* than detached systems. Furthermore, the inclination, and therefore the ratios of radii and luminosity, as well as whether the system undergoes complete eclipse are much better determined. Candidate *SD* distance determination systems can therefore be selected for the desirable properties of having double-lined spectra and complete eclipses more reliably than can detached systems.

We have computed both *SD* and detached solutions to the 1459 eclipsing binary stars identified in the SMC by the OGLE collaboration (Udalski et al. 1998). This work follows our earlier paper on detached systems. By fitting simulated catalogs we estimate a success rate of 98 percent for finding acceptable converged solutions to *SD* configurations. Acceptance of an *SD* solution does not establish that a system surely is *SD*, as detached systems can mimic *SD* light-curves and vice-versa. However, we show that the system condition (detached or *SD*) can often (for about 1/3 of our simulated binaries) be determined from the ratio of residuals (*SS* ratio). Of the OGLE systems with both kinds of solution, 36 percent have *SS* ratios significantly different from unity, allowing morphological categorization. In particular, also requiring eccentricity consistent with zero, we find 36 systems that can be identified as being of the *SD* morphological type with reasonable reliability (although 7 of these are doubtful due to very large mass ratios or periods), such that future observations with large scale optics should lead to accurate distance determinations. As emphasized in Section 4, we anticipate a coming time when several tests will better sift through high quality light curves and velocities from large optics. Comparison of photometric and spectroscopic mass ratios will then settle most of the otherwise unclear decisions between detached and *SD* assignments.

Although we expected that most binaries selected as *SD* would be common normal Algols, the result is that only a small minority of our *SD*'s have light curves like those of common Algols. Indeed, inspection of the OGLE catalog reveals that systems with light-curves resembling those of classical Algols are virtually absent. Only two of our *SD* candidate binaries have solutions consistent with normal Algols. Basically the secondary stars have high surface brightnesses (*i.e.* are hot compared to those of normal Algols). This outcome could be a strongly positive one, as *SD*'s with bright secondaries will have stronger light curve solutions (with information from *two* deep eclipses) than ordinary Algols, while they may retain all the *SD* advantages mentioned in the Introduction. They also have moderate

luminosity ratios, and therefore greatly increased likelihood of their spectra being double-lined.

It could be that some of the 36 *SD* binaries actually are *OC*, as testing for the *OC* condition is beyond the scope of this paper and will be treated in future work. That outcome also could be advantageous, as *OC* configurations can have very well conditioned light curve solutions, perhaps even better than *SD*'s. *OC* binaries are rare at the high luminosities detectable by OGLE (although very common at much lower luminosity), yet discovery of just a few would be valuable help in finding the distance to the Magellanic Clouds.

The next step is to obtain spectra and accurate multi-band light curves of the more promising systems so as to confirm *SD* assignments via spectral types and improved light curve parameters, and also to observe radial velocities for absolute dimensions.

The authors are very grateful to Professor Bohdan Paczynski for suggestions that led to this project, and for reading the manuscript. We are indebted to the OGLE collaboration for making their data public domain, and hence projects like this possible. Finally we would like to thank the anonymous referee whose careful reading and comments significantly enhanced the papers clarity. This work was supported in part by NASA through a Hubble Fellowship grant from the Space Telescope Science Institute, which is operated by the Association of Universities for Research in Astronomy, Inc., under NASA contract NAS 5-26555 (for J.S.B.W.), and in part by NSF grants AST-9819787 and AST-9820314 to Professor Paczynski.

REFERENCES

Alcock, C., Allsman, R. A., Alves, D., Axelrod, T. S., Becker, A. C., Bennett, D. P., Cook, K. H., Freeman, K. C., Griest, K., Lacy, C. H. S., Lehner, M. J., Marshall, S. L., Minniti, D., Peterson, B. A., Pratt, M. R., Quinn, P. J., Rodgers, A. W., Stubbs, C. W., Sutherland, W., Welch, D. L. 1997, AJ, 114, 326

Fitzpatrick, E.L., Ribas, I., Guinan, E.F., Dewarf, L.E., Maloney, F.P., Massa, D. 2001, ApJ, in press, astro-ph/0010526

Fitzpatrick, E.L., Massa, D. 1999, ApJ, 525, 1011

Grison, P., Beaulieu, J.-P., Pritchard, J. D., Tobin, W., Ferlet, R., Vidal-Madjar, A., Guibert, J., Alard, C., Moreau, O., Tajahmady, F., Maurice, E., Prevot, L., Gry, C.; Aubourg, E., Bareyre, P., Brehin, S., Gros, M., Lachieze-Rey, M., Laurent, B., Lesquoy, E., Magneville, C., Milsztajn, A., Moscoso, L., Queinnec, F., Renault, C., Rich, J., Spiro,

M., Vigroux, L., Zylberajch, S., Ansari, R., Cavalier, F., Moniez, M. 1995, A&AS, 109, 447

Guinan, E.F., Fitzpatrick, E.L., Dewarf, L.E., Maloney, F.P., Maurone, P.A., Ribas, I., Pritchard, J.D., Bradstreet, D.H., Gimenez, A. 1998, Ap. J., 509, 21

Kopal, Z. 1954, Jodrell Bank Ann., Vol. I, p.37

Kopal, Z. 1955, Ann. d'Ap., 18, 379

Kurucz, R.L. 1991, Harvard Preprint 3348

Levenberg, K. 1944, Quarterly of Applied Mathematics, 2, 164

Marquardt, D. W. 1963, J. Soc. Indust. Appl. Math., 11, 431

Morgan, J. G. & Eggleton, P. P. 1979, MNRAS, 187, 661

Ostrov P.G. 2001, A&A, 380, 258

Ostrov P.G., Lapasset E., Morrell N.I. 2000, A&A, 356, 935

Ostrov P.G., Lapasset E., Morrell N.I. 2001, A&A, 377, 972

Paczynski, B. 1997, Invited talk, presented at The Extragalactic Distance Scale STScI May Symposium, astro-ph/9608094

Paczynski, B. 2000, Millennium Essay, Publications of the Astronomical Society of the Pacific, astro-ph/0005284

Ribas, I., Guinan, E.F., Fitzpatrick, E.L., Dewarf, L.E., Maloney, F.P., Maurone, P.A., Bradstreet, D.H., Gimenez, A., Pritchard, J.D. 2000, ApJ, 528, 692

Rucinski, R. 1969, AcA, 19, 245

Semeniuk, I. 2000 AcA, 50, 381

Udalski, A., Soszynski, I., Szymanski, M., Kubiak, M., Pietrzynski, Z., Wozniak, P., Zebrun, K. 1998 AcA, 48, 563

Van Hamme, W. 1993, AJ, 106, 2096

Wilson, R. E. 1979, Ap. J., 234, 1054

Wilson, R. E. 1990, Ap. J., 356, 613

Wilson, R. E. 1994, PASP, 106, 921

Wilson, R. E. 1998, "Computing Binary Star Observables", Department of Astronomy, University of Florida, Gainesville, FL, 1998 edition

Wilson, R. E. Biermann, P., 1976, Astron. Atsrophys, 48, 349

Wilson, R. E. Devinney, E. J., 1971, Ap. J., 166, 605

Wyithe, J. S. B., Wilson, R. E. 2001, Ap. J., 559, 260

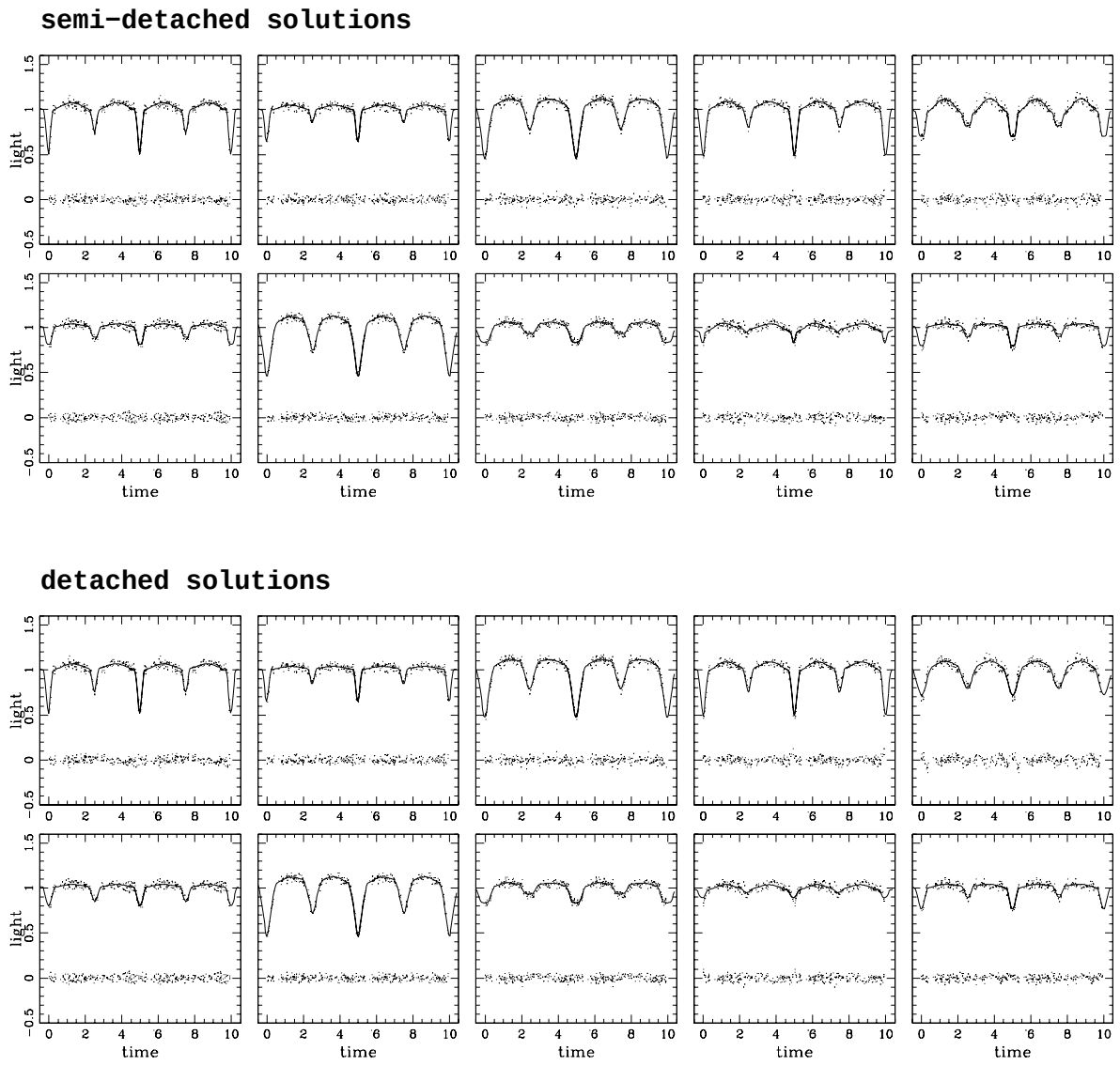

Fig. 1.— Examples of the simulated *SD* light curve data with corresponding solutions and residuals. Top: The solutions with *DC* in mode 5 (for *SD* condition). Bottom: The solutions with *DC* in mode 2 (for detached condition).

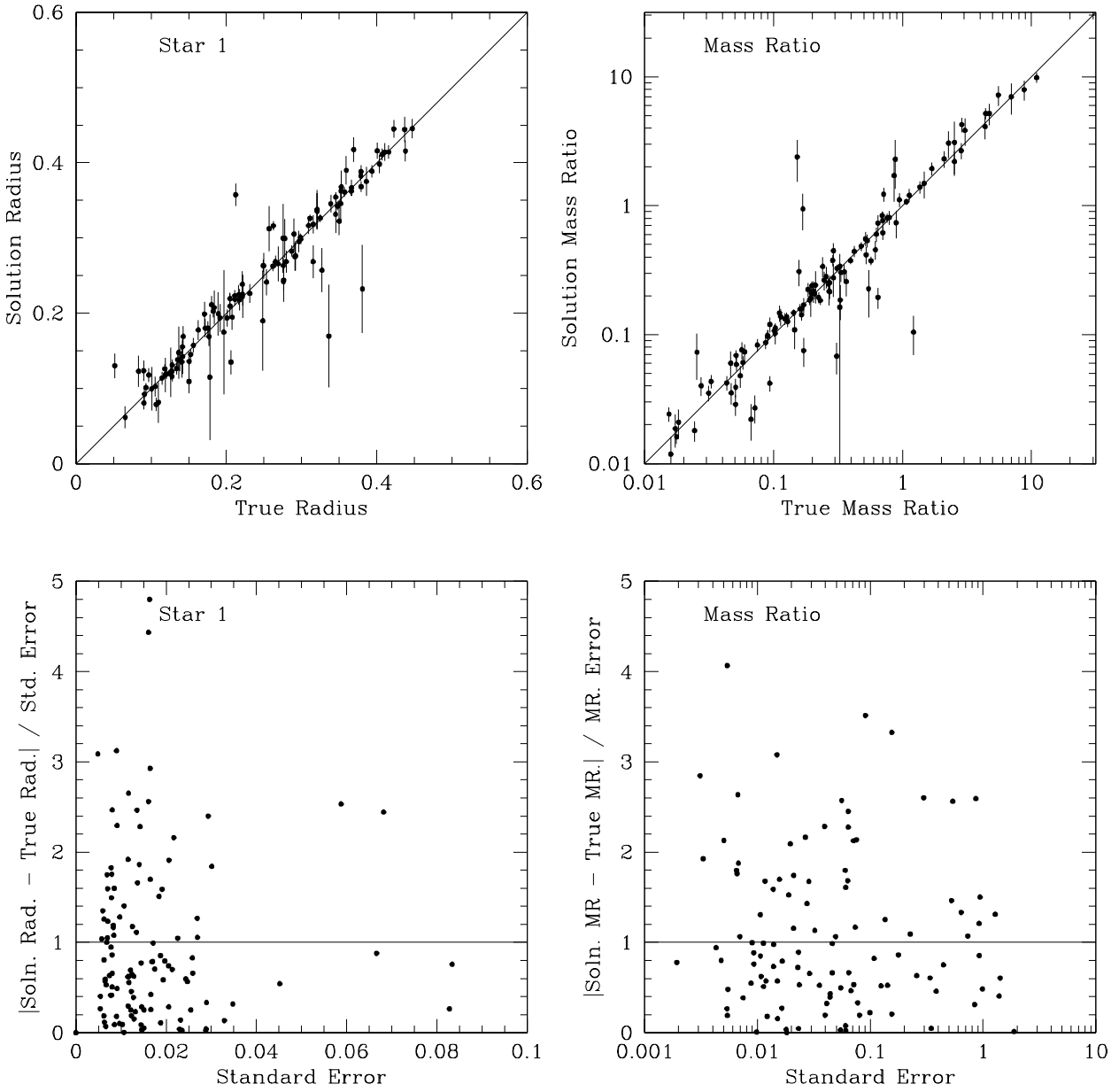

Fig. 2.— Top: r_1 (left) and q (right) (with standard errors Δr and Δq) from *SD* light curve solutions plotted against r_{sim} and q_{sim} for simulated *SD* binaries. The line of equality is drawn to guide the eye. Bottom left: $|r - r_{sim}|/\Delta r$ vs. Δr. Bottom right: $|q - q_{sim}|/\Delta q$ vs. the standard error Δq.

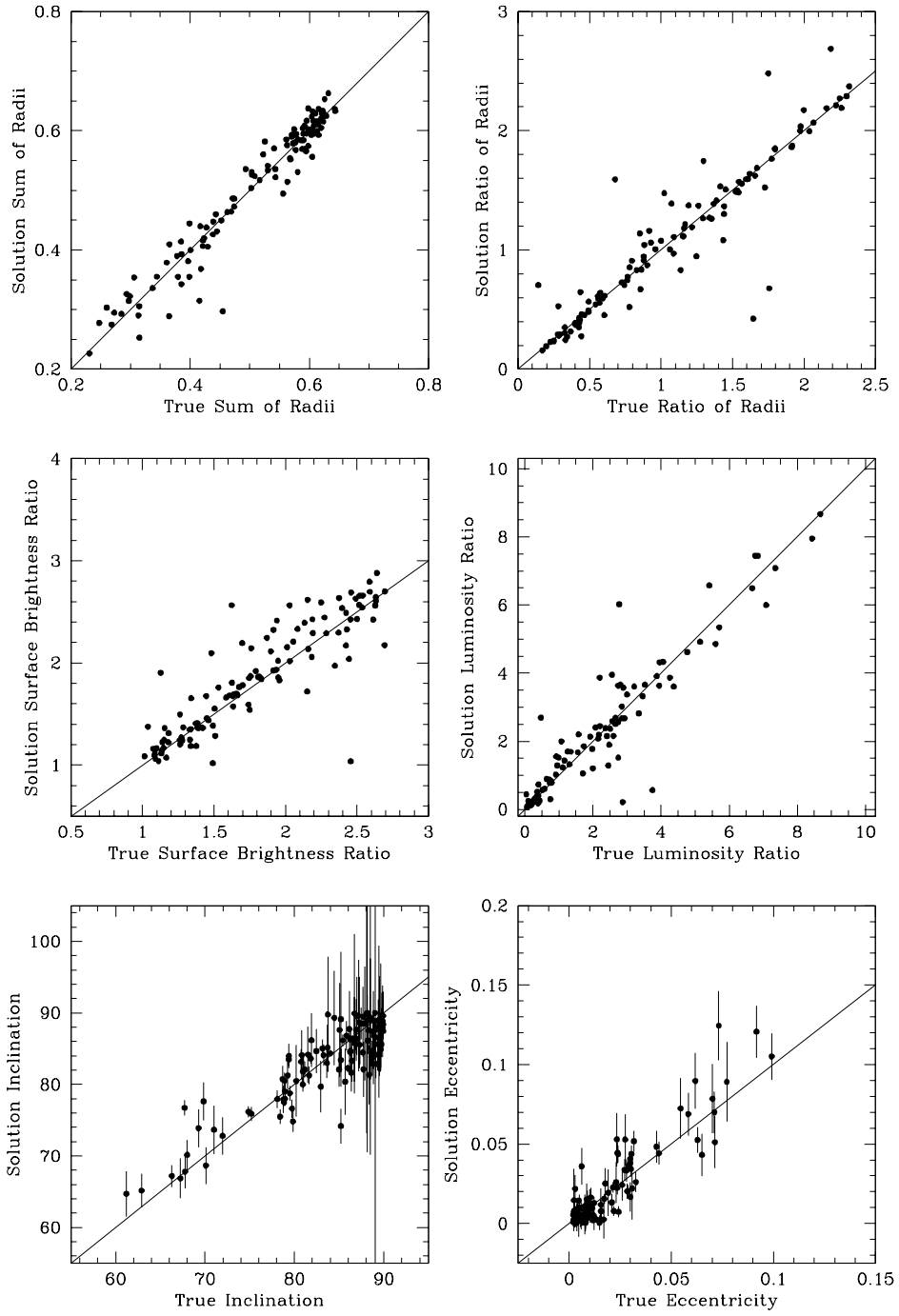

Fig. 3.— *SD* light curve parameters and combined quantities vs. simulated known values for simulated *SD* binaries. Plots are shown for $r_1 + r_2$, r_1/r_2, J_1/J_2, L_1/L_2, i, and e.

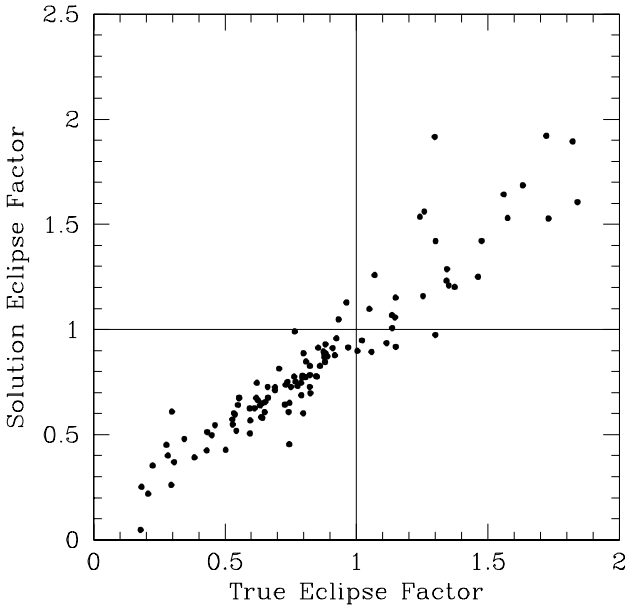

Fig. 4.— F_e from *SD* light curve solutions vs. that for the simulated *SD* eclipsing binaries, F_{sim}. The lines of unity are also drawn to separate regions of complete and incomplete eclipse.

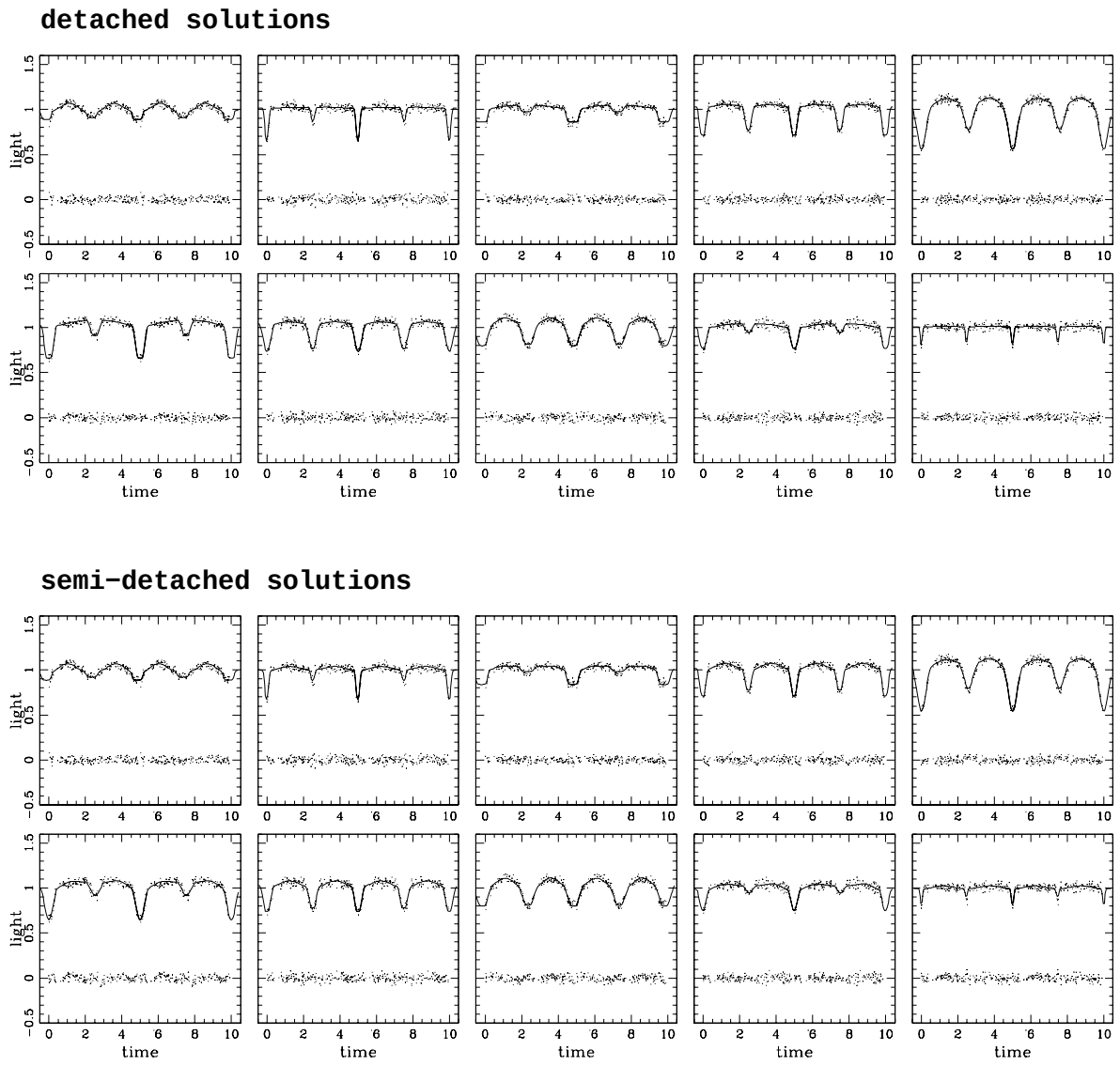

Fig. 5.— Examples of simulated detached light curve data with model light curves and residuals. Top: Solutions with *DC* in mode 2 (for detached condition). Bottom: Solutions with *DC* in mode 5 (for *SD* condition).

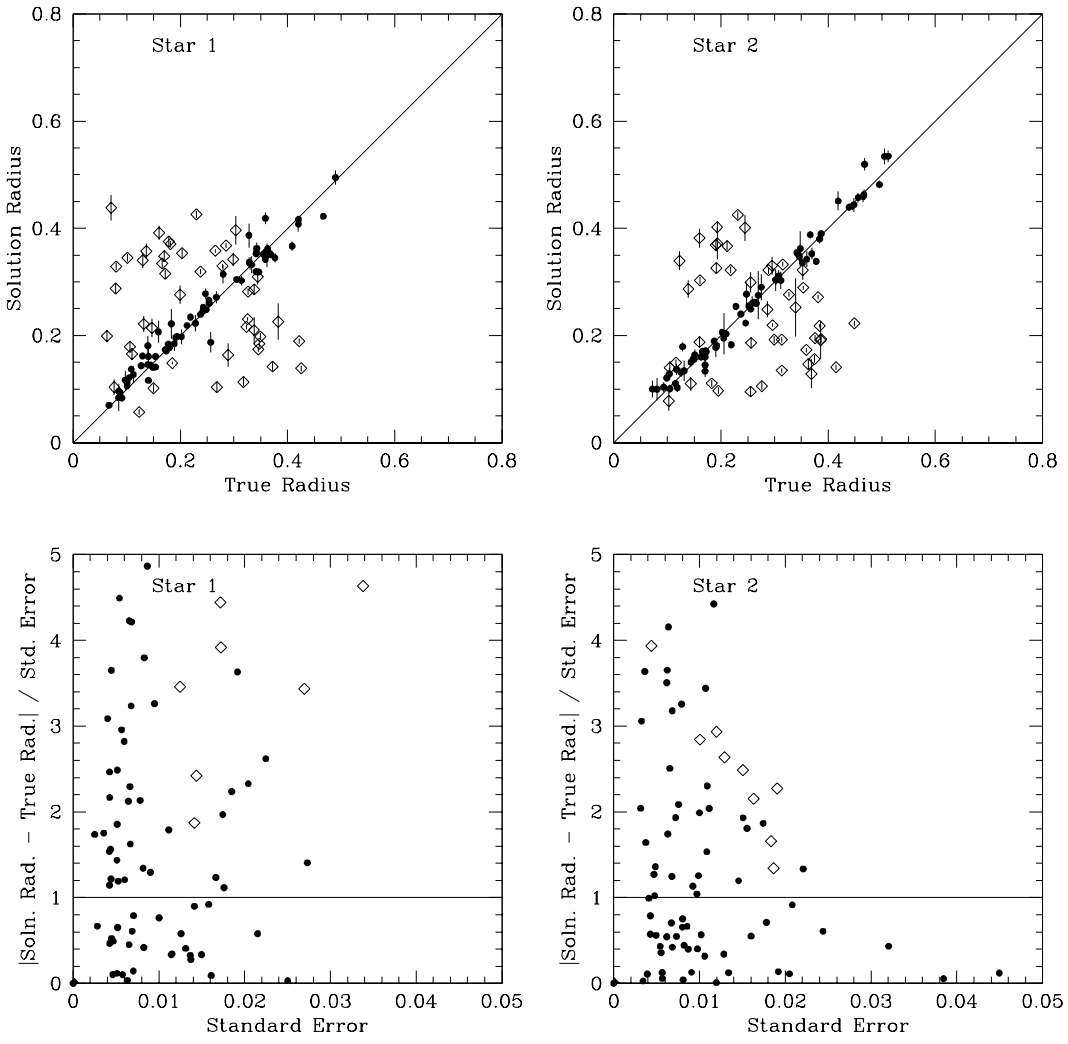

Fig. 6.— Top: r_1 (left) and r_2 (right) (with standard error, Δr) from light curve solutions vs. r_{sim} for simulated detached binaries. The line of equality is also drawn. Bottom: $|r - r_{sim}|/\Delta r$ vs. standard error Δr. (left: Star 1, right: Star 2). Diamonds show points for which the ratio of radii is inverted with respect to the correct value, and both radii differ significantly from the known values (aliased solutions).

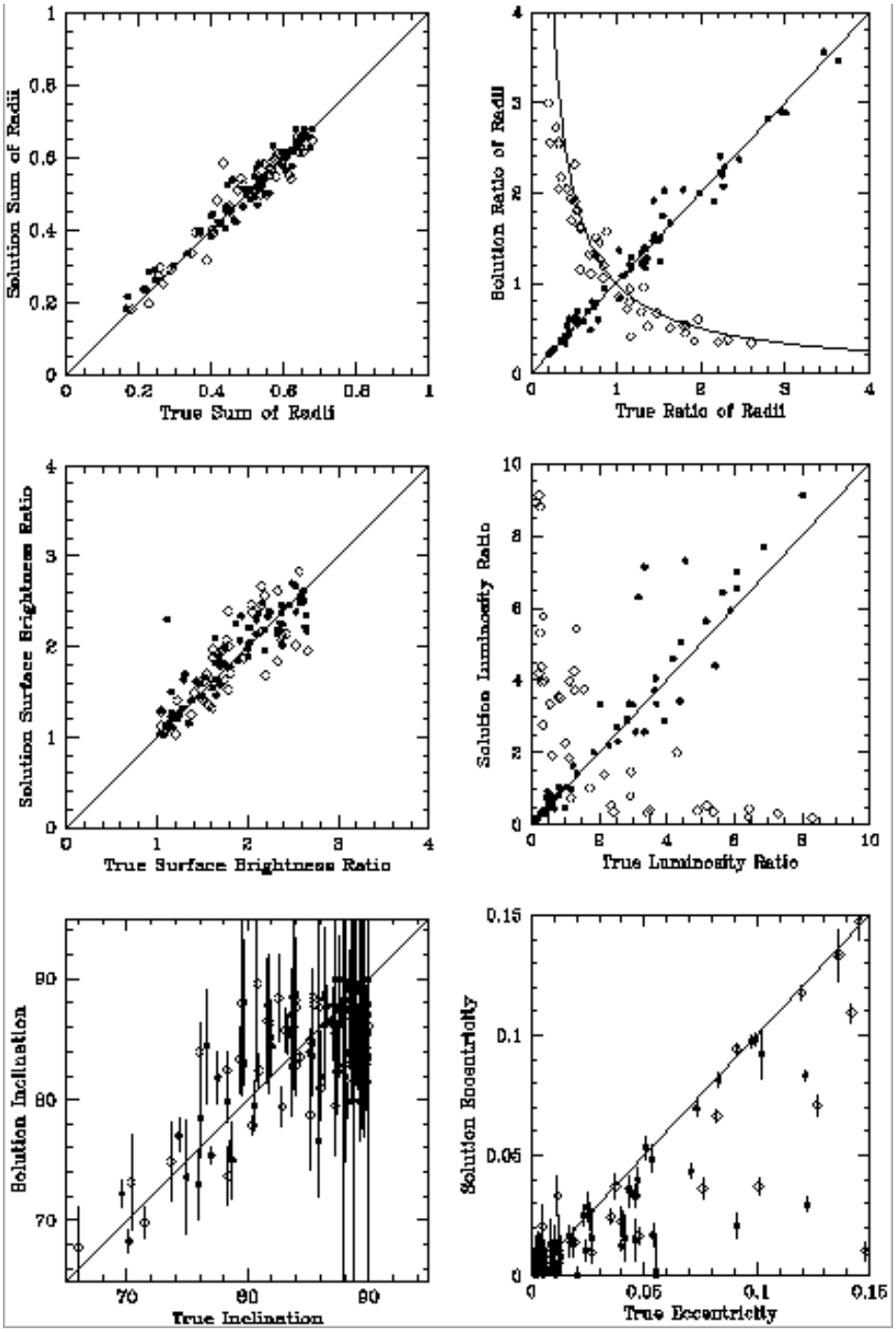

Fig. 7.— Light curve solution parameters with standard errors vs. known correct values for simulated detached binaries. Plots are for r_1 vs. r_2, r_1/r_2, J_1/J_2, L_1/L_2, i, and e. Diamonds show points where the ratio of radii is inverted with respect to the simulated system and both radii differ significantly from known values (aliased solutions). The *aliased* line $y = 1/x$ is shown to guide the eye.

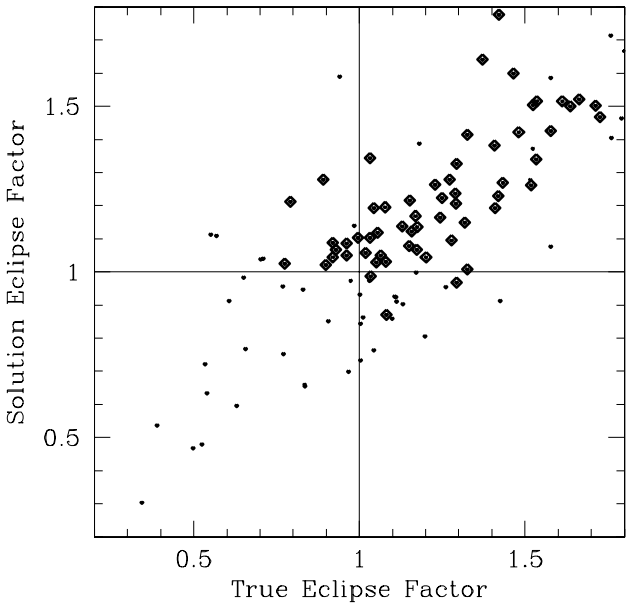

Fig. 8.— F_e's from the light curve solution vs. those for simulated detached binaries (F_{sim}). The lines of unity are drawn to separate regions of complete and partial eclipse. Cases where $\Delta r_1/r_1 < 0.05$ and $\Delta r_2/r_2 < 0.05$ are denoted by larger dots.

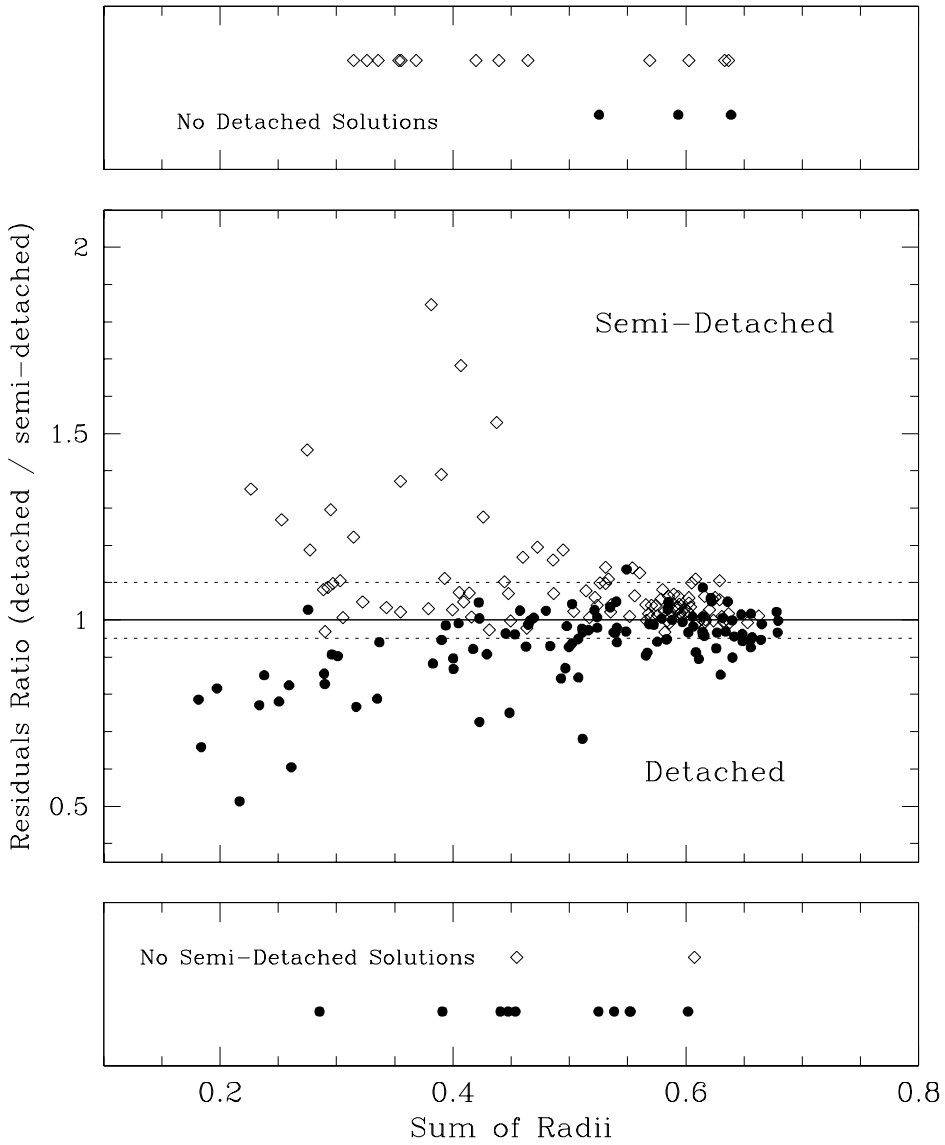

Fig. 9.— Central panel: *SS* ratio for detached to *SD* catalog solutions vs. $r_1 + r_2$. Diamonds are for the *SD* catalog and dots for the detached catalog. Horizontal dashed lines at 0.95 and 1.10 essentially bound the region of uncertain classification. Lower panel: Simulated systems having only a detached solution. Diamonds show misclassified objects. Upper panel: Simulated systems having only an *SD* solution, with dots for misclassified objects.

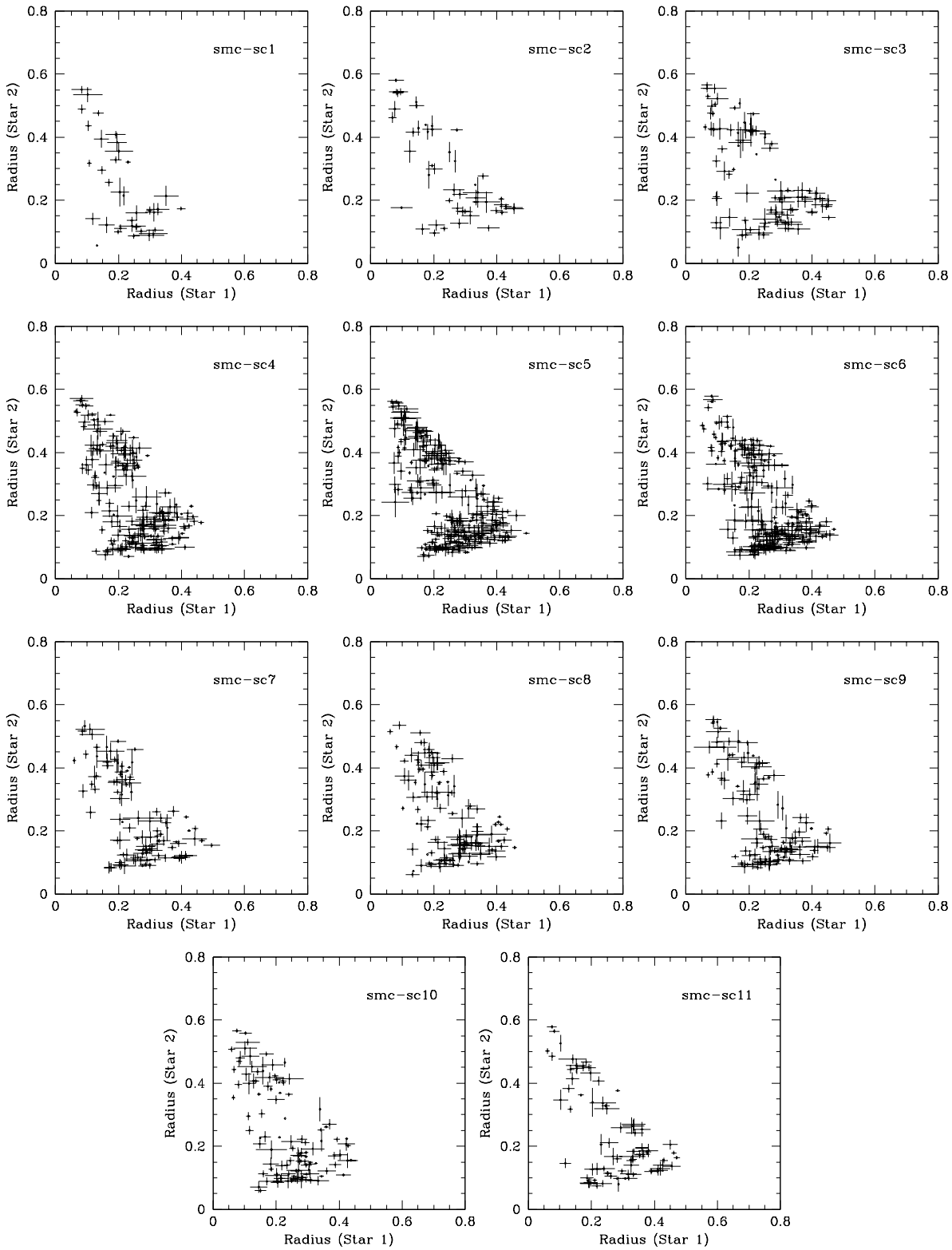

Fig. 10.— *SD* OGLE solutions for r_1 vs. r_2. Only error bars smaller than 0.05 are shown.

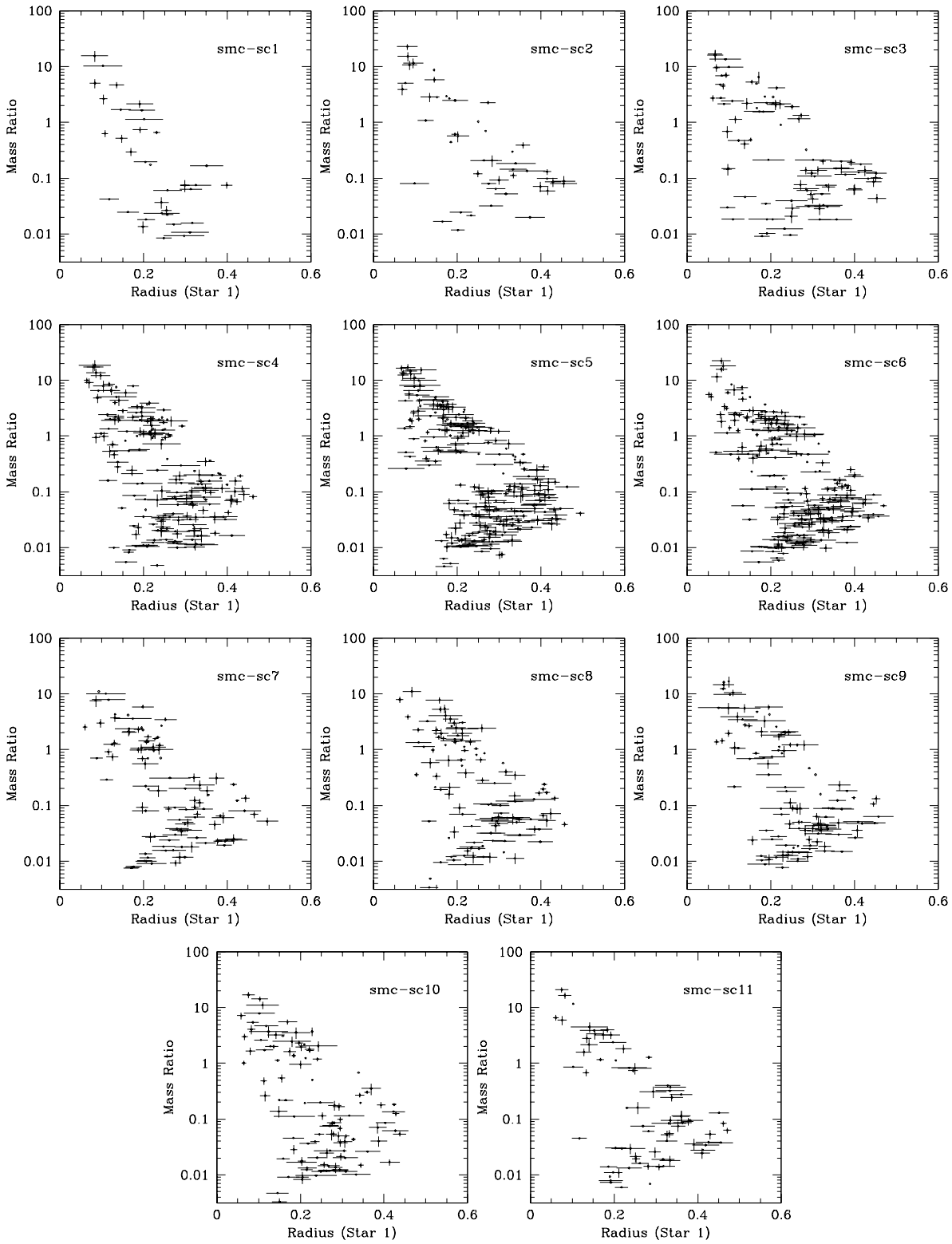

Fig. 11.— q vs. r_1 for *SD* OGLE solutions. Only fractional error bars in q smaller than 0.25, and in r_1 smaller than 0.05, are shown.

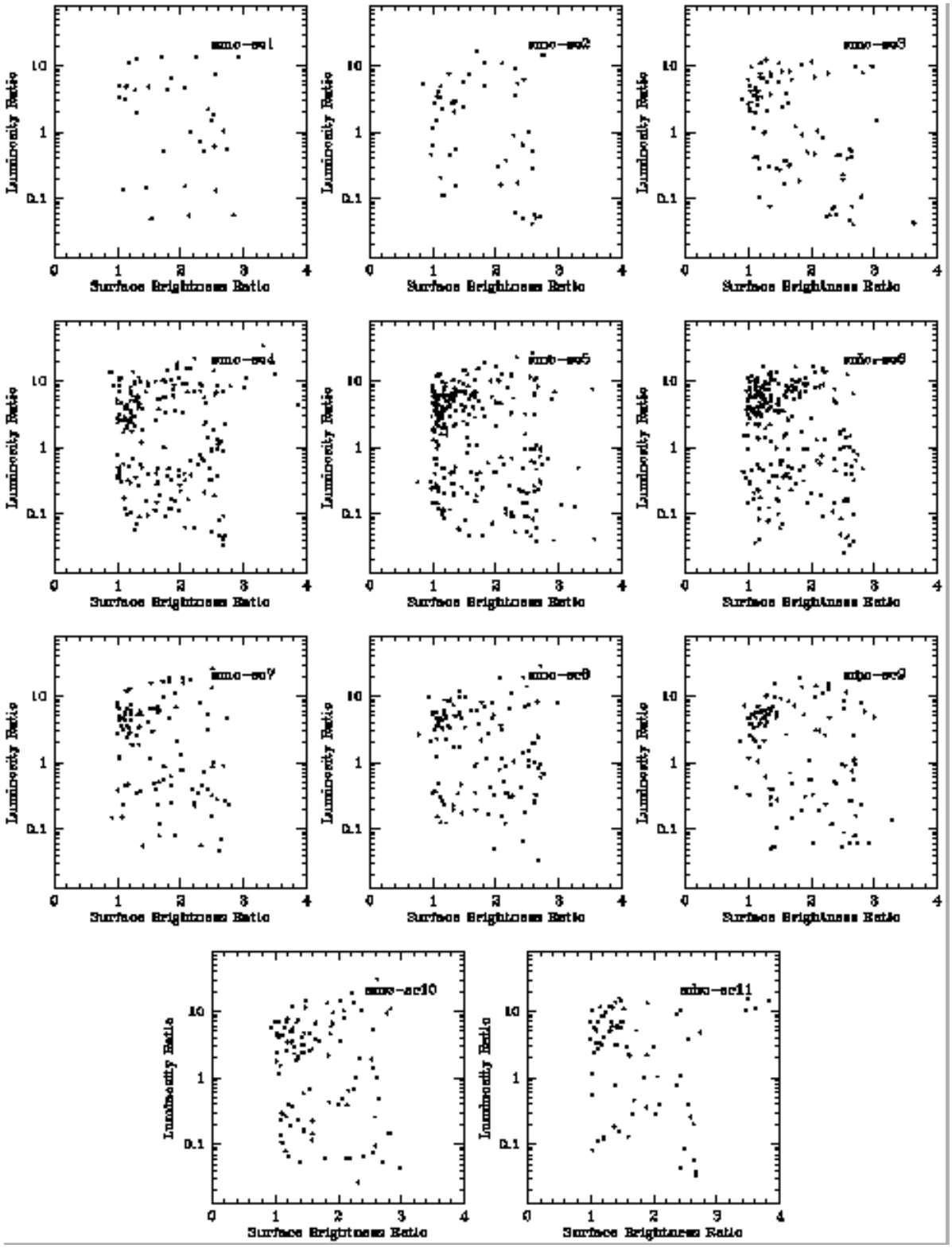

Fig. 12.— *SD* solutions for L_1/L_2 vs. J_1/J_2.

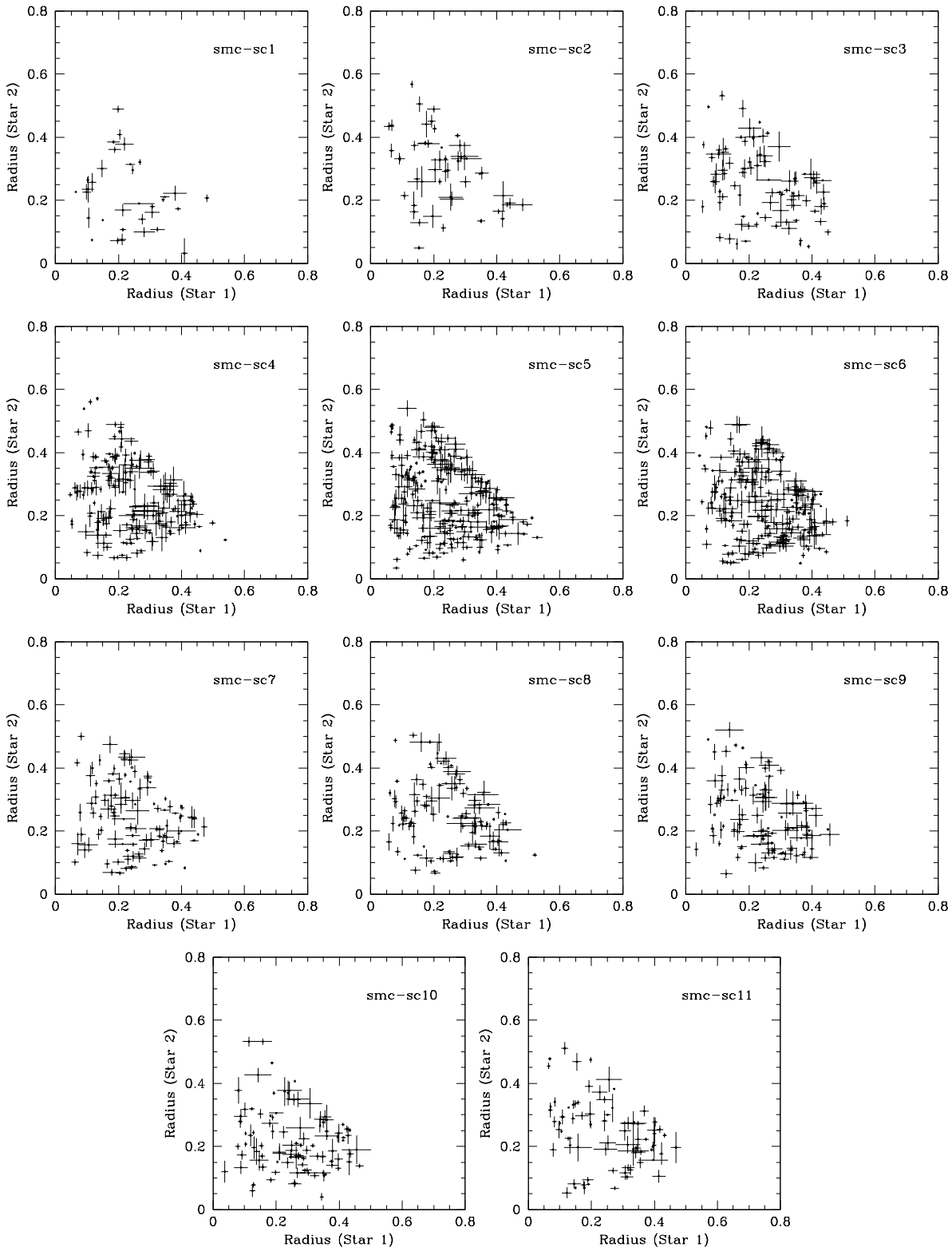

Fig. 13.— Detached solutions for r_1 vs. r_2. Only error bars smaller than 0.05 are shown.

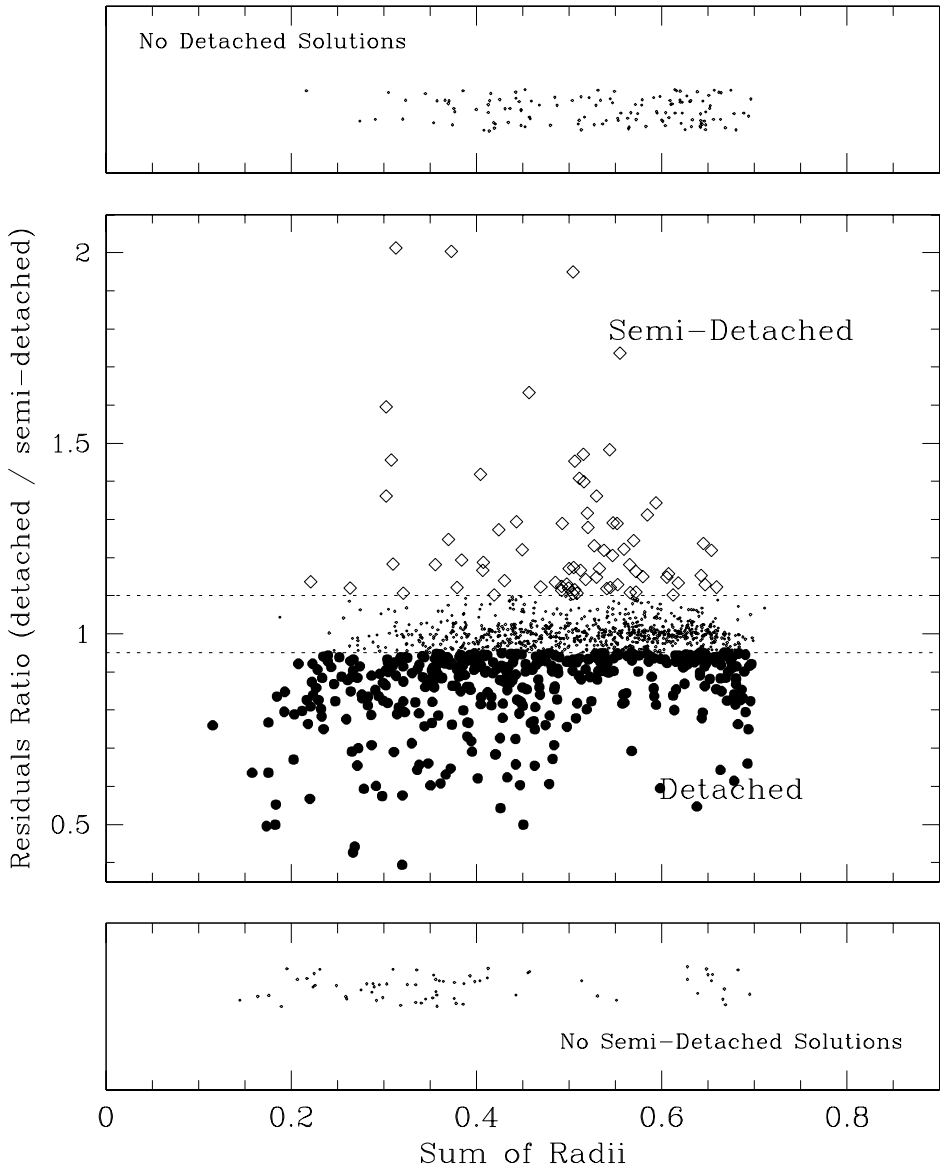

Fig. 14.— Central panel: *SS* ratio for detached to *SD* solutions of OGLE stars vs. $r_1 + r_2$. Diamonds show *SD* candidates and large dots detached candidates. Horizontal dashed lines at 0.95 and 1.10 delimit the uncertain region. Lower panel: Systems with only a detached solution. Upper panel: Systems with only a *SD* solution. The random scatter in the upper and lower panels has been introduced for clarity.

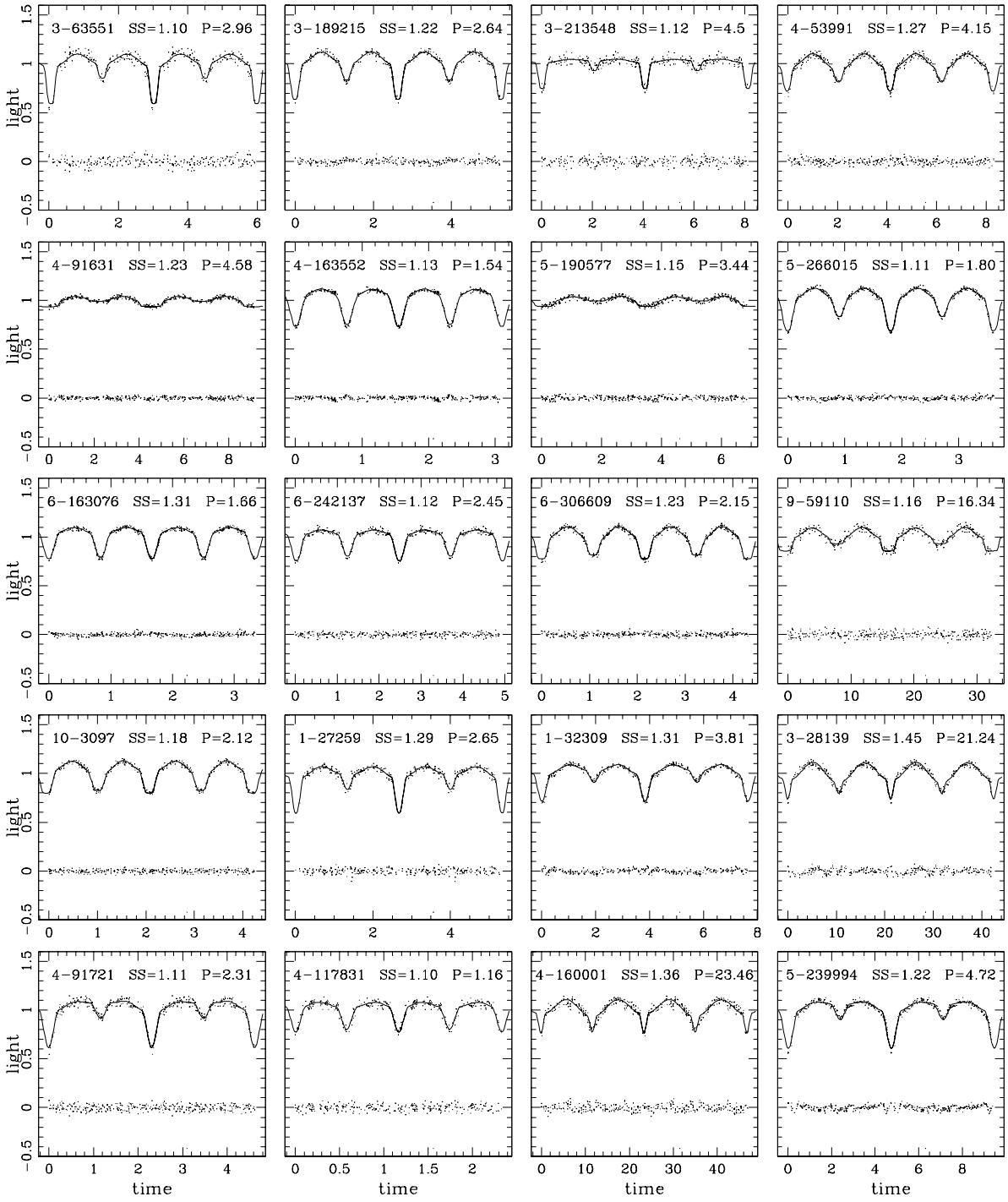

Fig. 15.— Light-curve fits for likely *SD* OGLE eclipsing binaries. Each panel is labeled by the OGLE field and object identification number, as well as the *SS* ratio and period. The solution parameters are in Tab. 4.

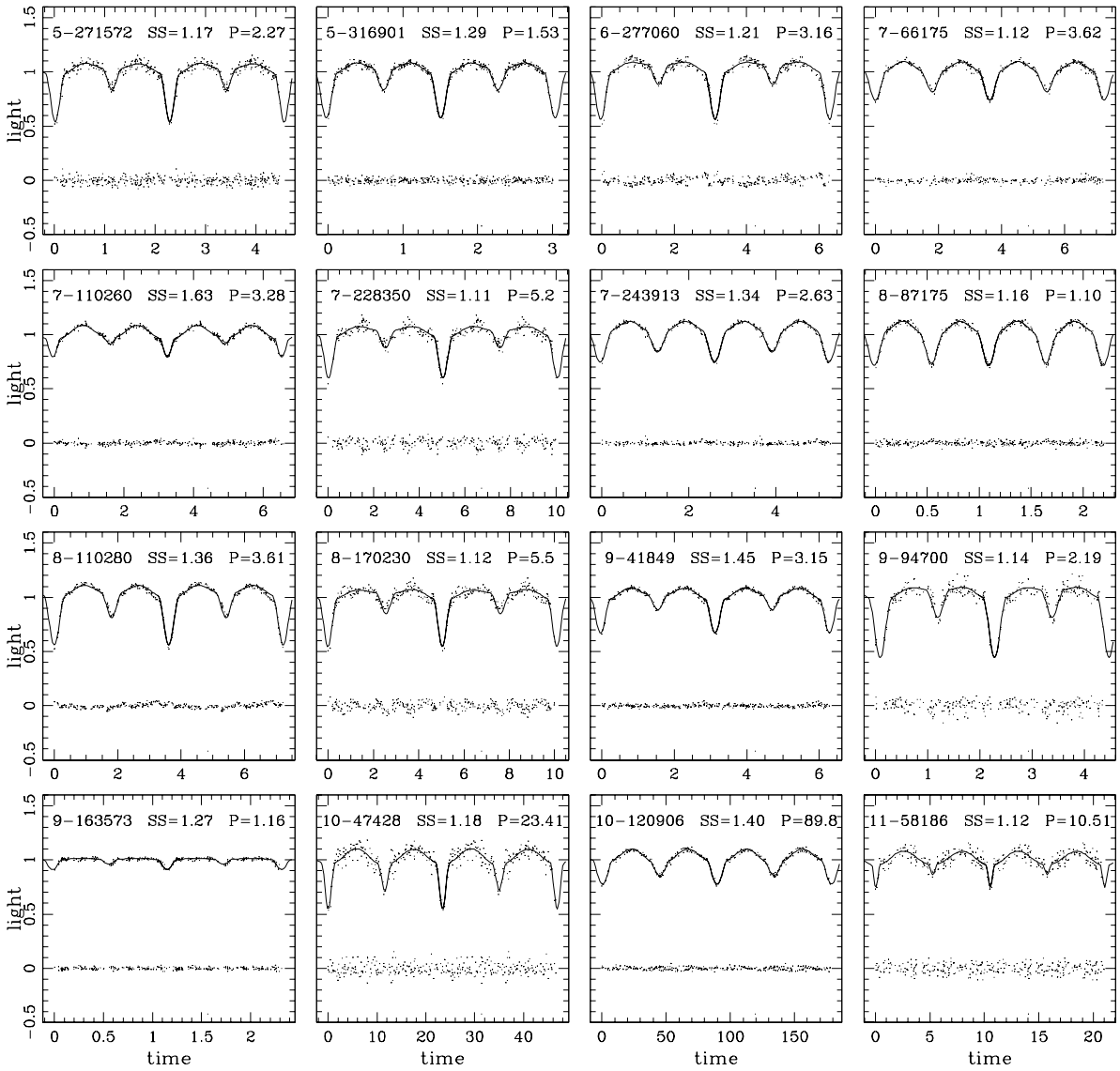

Fig. 16.— Continuation of Fig. 15.

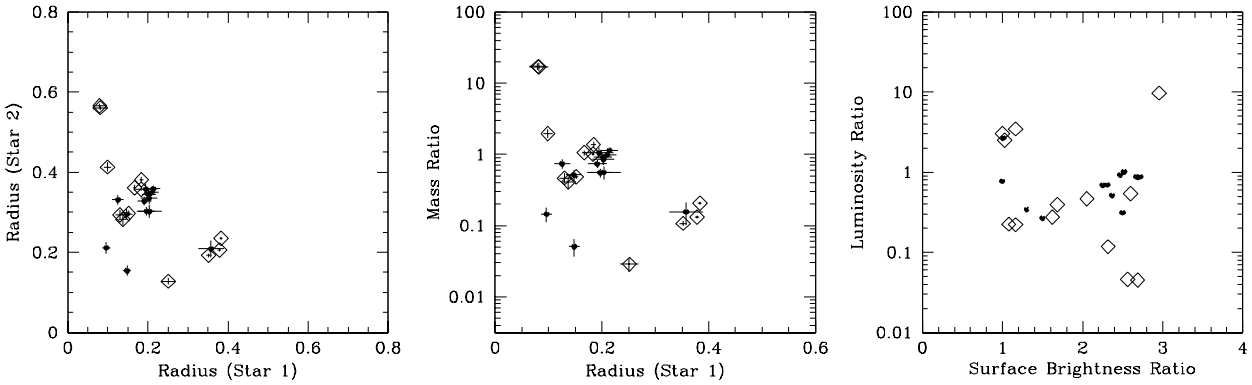

Fig. 17.— Solutions for the candidate *SD* catalog. Left: r_2 vs. r_1. Center: q vs. r_1. Right: L_1/L_2 vs. J_1/J_2. Only standard errors in radius smaller than 0.05 and in q (fractional errors) smaller than 0.25 are plotted. The dots and diamonds designate partially and completely eclipsing binaries respectively.

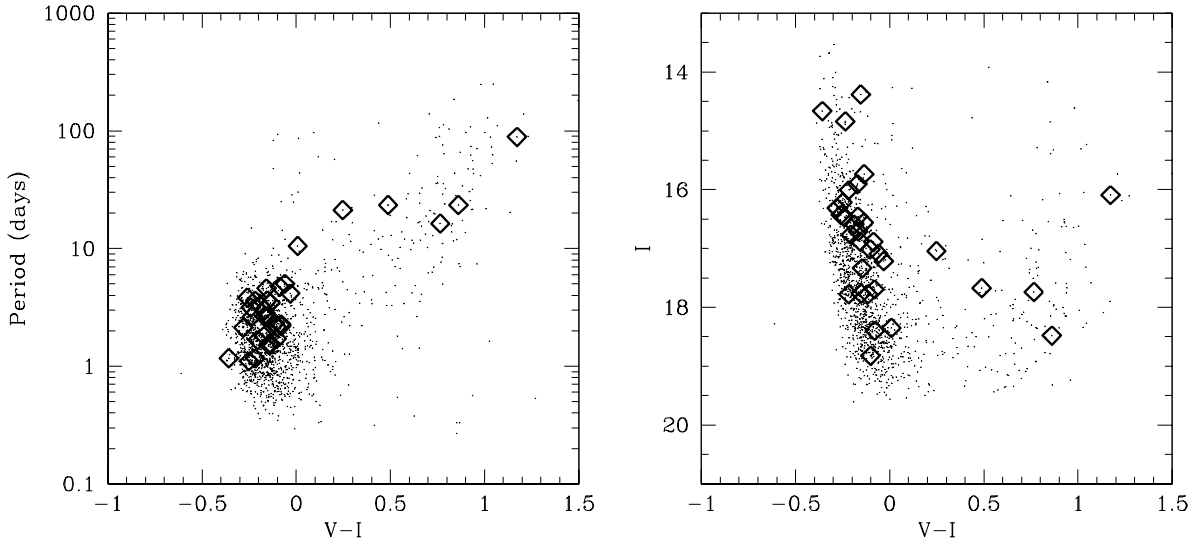

Fig. 18.— Color - period and color - magnitude diagrams for the full eclipsing binary catalog (small dots, data from Udalski et al. 1998). The *SD* objects are superimposed as diamonds. The V-I colors have been de-reddened assuming E(V-I)=0.14.

Mode 2

Group 1

subset 1	subset 2	subset 3
e	i	T_1
Ω_1	L_1	t_0
Ω_2		

Group 2

subset 1	subset 2	subset 3
e	i	T_1
t_0	Ω_2	Ω_1
L_1		

Mode 5

Group 1

subset 1	subset 2	subset 3
e	i	T_1
Ω_1	L_1	t_0
q		

Group 2

subset 1	subset 2	subset 3
e	i	T_1
t_0	q	Ω_1
L_1		

Group 3

subset 1	subset 2	subset 3
Ω_1	i	T_1
q	L_1	t_0

Group 4

subset 1	subset 2	subset 3
t_0	i	T_1
L_1	q	Ω_1

Table 1: Table showing the groups of subsets used by dc in modes 2 (top) and 5 (bottom).

parameter	description
i (adjusted*)	binary orbit inclination (degrees).
T_1 (adjusted*)	mean surface effective temp. (K) of star 1.
L_1 (adjusted*)	luminosity for star 1.
t_0 (adjusted)	zero point of orbital ephemeris.
e (adjusted)	binary orbit eccentricity.
Ω_1 (adjusted*)	potential of star 1.
Ω_2 (in mode 2: adjusted*)	potential of star 2.
Ω_2 (in mode 5: set by q)	potential of star 2.
q (in mode 2: set from initial guess)	mass ratio.
q (in mode 5: adjusted*)	mass ratio.
ω= 0.0 or π (in mode 2: set from initial guess)	argument of periastron for star 1.
$0 < \omega < \pi$ (in mode 5: set from initial guess)	argument of periastron for star 1.
$T_2 = 10000.0$	mean surface effective temp. (K) of star 2.
L_2 (set from initial guess)	luminosity for star 2.
P (from Udalski et al.)	period of binary orbit (days).
λ_I= 0.9	wavelength of light curve in microns.
$x_1 = 0.32$	linear limb darkening coefficient of star 1.
$x_2 = 0.32$	linear limb darkening coefficient of star 2.
$y_1 = 0.18$	non-linear limb darkening coefficient of star 1.
$y_2 = 0.18$	non-linear limb darkening coefficient of star 2.
$l_3 = 0.0$	third light.
$f_1 = 1.0$	ratio of axial rotation rate to mean orbital rate.
$f_2 = 1.0$	ratio of axial rotation rate to mean orbital rate.
$g_1 = 1.0$	exponent in gravity brightening (bolo. flux prop. to local gravity).
$g_2 = 1.0$	exponent in gravity brightening (bolo. flux prop. to local gravity).
$A_1 = 1.000$	bolometric albedo of star 1.
$A_2 = 1.000$	bolometric albedo of star 2.
$\lambda = 10^{-5}$	the Marquardt multiplier.

Table 2: Table of parameters with descriptions. The adjusted parameters are labeled as such (those for which convergence is required are also marked by *), and the values of fixed parameters are given. Note that g should not be confused with surface gravity.

control integer	description
NREF = 1	number of reflections.
MREF = 1	simple reflection treatment.
LD = 2	logarithmic limb darkening law.
JDPHS = 1	independent variable time.
NOISE = 1	scatter scales with sqrt (light level).
MODE = 2 or 5	mode of program operation.
IPB = 0	for normal operation in mode 2.
IFAT1 = 0	for black body (star 1).
IFAT2 = 0	for black body (star 2).
N1 = 30	grid size for star 1.
N2 = 30	grid size for star 2.
N1L = 15	coarse grid integers for star 1.
N2L = 15	coarse grid integers for star 2.
IFVC1 = 0	no radial velocity curve for star 1.
IFVC2 = 0	no radial velocity curve for star 2.
NLC = 1	number of light-curves.
KDISK = 0	no scratch pad.
ISYM = 1	use symmetrical derivatives.

Table 3: Table of control integers with descriptions (nomenclature from Wilson 1998).

Field	Object	q	$\frac{R_1}{a}$	$\frac{R_2}{a}$	$\frac{J_1}{J_2}$	i (degrees)	e	$\frac{L_1}{L_2}$	F_e	Period	I	V-I
3	63551	0.412 ± 0.077	0.137 ± 0.010	0.282±0.014	2.599	84.1 ± 1.8	0.012 ± 0.015	0.54	1.151	2.9691	16.7090	-0.0280
3	189215	0.487 ± 0.040	0.151 ± 0.005	0.298 ±0.006	2.054	83.3 ± 0.8	0.000 ± 0.002	0.47	1.099	2.6424	16.4560	-0.0290
3	213548	0.029 ± 0.006	0.251 ± 0.017	0.128 ±0.009	2.958	88.4 ± 6.3	0.013 ± 0.007	9.73	1.374	4.0572	17.9280	0.3000
4	53991	0.468 ± 0.071	0.130 ± 0.010	0.294 ±0.012	1.625	80.8 ± 1.2	0.002 ± 0.006	0.28	1.020	4.1593	17.2130	0.1080
4	91631†	17.142 ± 1.912	0.080 ± 0.015	0.565 ±0.006	2.686	84.7 ± 3.6	0.000 ± 0.003	0.05	3.455	4.5871	16.8760	-0.0180
4	163552	0.207 ± 0.010	0.383 ± 0.004	0.234 ±0.003	1.027	82.8 ± 0.7	0.004 ± 0.002	2.52	1.050	1.5458	15.7350	0.0040
5	190577†	17.026 ± 2.233	0.082 ± 0.018	0.561 ±0.007	2.564	76.2 ± 3.3	0.013 ± 0.007	0.05	2.476	3.4405	16.5630	0.0030
5	266015	1.014 ± 0.051	0.183 ± 0.003	0.357 ±0.004	1.685	80.8 ± 0.4	0.000 ± 0.002	0.39	1.037	1.8089	15.9020	-0.0320
6	163076	0.132 ± 0.007	0.378 ± 0.004	0.206 ±0.003	0.998	81.5 ± 0.7	0.003 ± 0.003	3.04	1.058	1.6684	16.7660	-0.0660
6	242137	0.108 ± 0.009	0.352 ± 0.007	0.192 ±0.005	1.162	81.5 ± 1.0	0.013 ± 0.006	3.47	1.032	2.4572	17.2040	-
6	306609	1.061 ± 0.089	0.167 ± 0.004	0.361 ±0.007	1.165	90.0 ± 14.9	0.002 ± 0.002	0.22	1.580	2.1532	17.0150	0.0370
9	59110 ∗	1.963 ± 0.276	0.099 ± 0.009	0.413 ±0.012	2.320	89.7 ± 5.9	0.001 ± 0.002	0.12	2.564	16.3409	17.7390	0.9050
10	3097	1.374 ± 0.128	0.184 ± 0.005	0.381 ±0.008	1.077	85.1 ± 1.4	0.005 ± 0.002	0.23	1.303	2.1284	16.3150	-0.1410
1	27259	0.517 ± 0.088	0.147 ± 0.014	0.296 ±0.013	2.366	81.0 ± 1.3	0.028 ± 0.012	0.52	0.976	2.6569	17.7680	-0.0120
1	32309	0.739 ± 0.097	0.191 ± 0.018	0.328 ±0.011	2.311	73.6 ± 0.4	0.011 ± 0.005	0.70	0.620	3.8188	16.4290	-0.1200
3	28139∗	0.146 ± 0.034	0.096 ± 0.011	0.211 ±0.014	1.499	81.3 ± 0.6	0.007 ± 0.004	0.27	0.812	21.2494	17.0440	0.3880
4	91721	1.143 ± 0.110	0.214 ± 0.016	0.359 ±0.008	2.686	74.9 ± 0.7	0.032 ± 0.013	0.87	0.731	2.3136	17.7780	0.0250
4	117831	0.157 ± 0.054	0.357 ± 0.032	0.209 ±0.021	1.010	77.9 ± 2.1	0.049 ± 0.019	2.69	0.852	1.1645	17.7790	-0.0780
4	160001∗	0.051 ± 0.014	0.148 ± 0.010	0.155 ±0.013	0.996	81.3 ± 0.6	0.002 ± 0.004	0.78	0.513	23.4661	17.6730	0.6280
5	239994	0.996 ± 0.102	0.210 ± 0.018	0.349 ±0.008	2.719	75.5 ± 0.5	0.024 ± 0.009	0.88	0.737	4.7274	16.8870	0.0530
5	271572	0.553 ± 0.077	0.197 ± 0.021	0.303 ±0.011	2.468	80.1 ± 0.6	0.019 ± 0.008	0.92	0.834	2.2733	17.6940	0.0590
5	316901	0.912 ± 0.120	0.202 ± 0.018	0.345 ±0.011	2.252	79.3 ± 0.7	0.011 ± 0.008	0.69	0.894	1.5304	17.3330	-0.0060
6	277060	0.848 ± 0.142	0.203 ± 0.021	0.335 ±0.014	2.671	78.2 ± 0.7	0.030 ± 0.014	0.88	0.821	3.1612	16.4920	-
7	66175	1.060 ± 0.193	0.195 ± 0.027	0.358±0.015	1.303	76.8 ± 1.5	0.012 ± 0.008	0.34	0.833	3.6264	14.3820	-0.0140
7	110260	0.744 ± 0.111	0.125 ± 0.015	0.311 ±0.012	2.497	72.5 ± 0.5	0.001 ± 0.003	0.31	0.620	3.2881	16.5900	-0.0500
7	228350	0.560 ± 0.120	0.204 ± 0.031	0.302 ±0.017	2.517	77.3 ± 0.9	0.027 ± 0.015	1.02	0.703	5.0240	17.0900	0.0810
7	243913	1.447 ± 0.134	0.208 ± 0.019	0.386 ±0.008	1.365	76.5 ± 1.3	0.004 ± 0.006	0.36	0.869	2.6316	14.8400	-0.0960
8	87175	0.968 ± 0.076	0.218 ± 0.009	0.354 ±0.006	1.005	81.8 ± 1.1	0.001 ± 0.001	0.34	0.985	1.1022	16.2200	-0.1100
8	110280	0.655 ± 0.053	0.210 ± 0.010	0.320 ±0.006	2.048	81.3 ± 0.4	0.007 ± 0.007	0.79	0.899	3.6153	16.0050	-0.0770
8	170230	0.384 ± 0.074	0.220 ± 0.021	0.272 ±0.014	2.512	79.8 ± 0.7	0.035 ± 0.013	1.46	0.716	5.0538	17.2660	0.1880
9	41849	0.867 ± 0.054	0.164 ± 0.008	0.342 ±0.005	2.387	76.1 ± 0.4	0.010 ± 0.005	0.49	0.812	3.1590	16.4650	-0.1010
9	94700	0.958 ± 0.206	0.231 ± 0.030	0.348 ±0.018	2.677	83.1 ± 2.0	0.017 ± 0.016	1.07	0.992	2.1934	18.3980	0.0610
9	163573	0.026 ± 0.007	0.402 ± 0.018	0.118 ±0.011	1.831	72.0 ± 2.5	0.076 ± 0.032	18.8	0.895	1.1670	14.6640	-0.2180
10	47428∗	0.138 ± 0.032	0.148 ± 0.021	0.207 ±0.014	1.539	85.5 ± 1.1	0.011 ± 0.006	0.68	0.936	23.4192	18.4770	1.0010
10	120906∗	1.129 ± 0.076	0.145 ± 0.006	0.366 ±0.006	1.592	76.6 ± 0.8	0.002 ± 0.003	0.22	0.962	89.0876	16.0910	1.3120
11	58186∗	0.045 ± 0.015	0.117 ± 0.018	0.146 ±0.016	1.835	81.0 ± 1.0	0.022 ± 0.023	1.01	0.459	10.5115	18.3500	0.1480

Table 4: Table of parameters for *SD* eclipsing binaries. Those having complete eclipses are shown in the upper section, and those having partial eclipses in the lower section of the table. The periods (in days), I-magnitudes and colors are taken from Udalski et al. (1998). The binaries marked by †'s are doubtful due to very large mass ratios, and those marked by an $*$ are doubtful due to long periods.